Physics – Uspekhi **43** (2) 111 – 137 (2000)

REVIEWS OF TOPICAL PROBLEMS

PACS numbers: **36.40.+d**, **61.46.+w**, **61.48.+c**, **85.42.+m**

Endohedral structures

A V Eletskiĭ

DOI: 10.1070/PU2000v043n02ABEH000646

Contents

Abstract. A review is presented of the current knowledge of endohedral structures — fullerene molecules and carbon nanotubes with one or more atoms inside. Methods of synthesis and exploration of such structures are considered and the results obtained are discussed. The charge state and the geometrical position of atoms encapsulated inside the fullerene molecules and the chemical properties of the resulting endohedral compounds are analyzed. The recent development of methods for producing macroscopic quantities of such molecules in a pure form has resulted in the formation of a new area of research aimed at the determination of the characteristics and physical and chemical properties of matter consisting of endohedral fullerene molecules. The results of such investigations and prospects for further development in this field are analyzed.

1. Introduction

Analyzing the development of areas of physical and chemical research related to the study of microscopic objects, one could note a change in the character of such a research, which has been exhibited most strikingly during the last decades. Whereas in the past an atomic particle (atom, ion, molecule) of natural origin served as the main subject of investigation, at present submicron- and nanometer-size objects of artificial origin are put in the forefront. Clusters, quantum dots, superlattices, etc. are typical examples. This situation can be characterized as a transition from the analysis to the synthesis of physical objects, which should undoubtedly be considered as an indicator of a qualitative development of the scientific branch. The present article concerns endohedral structures, which are one of the most significant examples of artificially designed objects.

The discovery of fullerenes in 1985 [1 – 4], awarded with the Nobel Prize for Chemistry in 1996, is one of the notable scientific advances of the passing century. Fullerenes are closed surface carbon structures of high chemical stability, in which the carbon atoms are situated at the vertices of regular hexagons or pentagons, covering in a regular manner the surface of a sphere or spheroid. The most abundant fullerene molecule C_{60} has the structure of a regular truncated icosahedron whose surface consists of twelve pentagons and twenty hexagons arranged so that each pentagon is adjacent to only hexagons, whereas each hexagon is adjacent to three pentagons and three hexagons alternately. The fullerene molecule C_{60} is of high symmetry so that the geometrical positions as well as the chemical states of all carbon atoms are fully equivalent. Each of the atoms of such a molecule belongs to one pentagon and two hexagons, which determines its chemical state and electronic structure. The class of fullerene molecules includes, along with C_{60}, larger molecules such as C_{70}, C_{76}, C_{84}, etc., which are characterized, however, by a considerably lower symmetry. The discovery of fullerenes stimulated further research efforts addressed to the synthesis and exploration of new carbon structures. The rise in activity of these efforts was stimulated by the work of Krätchmer and Huffman [5], who in 1990 developed the method of fullerene production in macroscopic quantities based on the use of an arc discharge with graphite electrodes. The family of artifi-

A V Eletskiĭ Russian Research Centre 'Kurchatov Institute'
Kurchatov square 1, 123182 Moscow, Russian Federation
Tel./Fax (7-095) 196-72 80
E-mail: eletskii@imp.kiae.ru

Received 30 July 1999
Uspekhi Fizicheskikh Nauk **170** (2) 113 – 142 (2000)
Translated by A V Eletskiĭ; edited by S N Gorin

cially synthesized carbon structures was supplemented with such new objects as carbon nanotubes, endohedral fullerenes, etc. in consequence of this discovery. The properties of fullerenes and some other carbon structures were considered in detail recently in *Physics – Uspekhi* [6 – 10].

The possibility of existence and ways of synthesis of fullerene molecules with one or several atomic particles incorporated inside of them follow from the unique structure of fullerene molecules which is in essence a hollow spherical or spheroidal shell. This possibility, which was actively considered in the literature immediately after the fullerene discovery [1], stems from the fact that the inner size of a fullerene cage (about 0.7 nm) considerably exceeds the characteristic effective diameter of atoms and simple molecules (0.1 – 0.4 nm). Fullerene molecules encapsulating one or several atomic particles (atoms or molecules) have been called endohedral compounds (or endohedrals). These compounds are symbolized by the formula $M_m@C_n$, where M is the encapsulated atom or molecule and the subscripts m and n show the number of such atoms and carbon atoms in the fullerene molecule, respectively. This notation permits us to distinguish between an endohedral molecule and conventional (exohedral) chemical compounds which (in the case of fullerenes) are designated by the standard symbol M_mC_n.

The first report about the synthesis and observation of endohedral fullerenes appeared soon after the discovery of fullerenes and belonged to the authors of this discovery [11]. However, the quantity of endohedrals synthesized in the first experiments was hardly sufficient even to detect the signal in a mass spectrometer. Such a low quantity of synthesized molecules cast natural doubts, whether the molecular structure corresponded to the position of an encapsulated atom inside the fullerene cage. More detailed questions concerning the specific position of an encapsulated particle, its charge state as well as properties of macroscopic bulk formations consisting of endohedral molecules seemed even harder to answer.

These doubts became possible to resolve only after the development of the method of synthesis, separation and purification of fullerenes in macroscopic quantities [5] in 1990. This method is based on the thermal sputtering of graphite electrodes in an arc discharge burning in a rare gas atmosphere (helium or argon). This results in the formation of a soot, containing up to 20% fullerene C_{60} and C_{70} with a small admixture of heavy fullerenes. The subsequent extraction of fullerenes from the soot is based on the fact that the fullerenes, as distinct from other carbon modifications, are soluble in a variety of solvents (benzene, toluene, xylene, CS_2, etc.). This permits separating the fullerenes from other components of the soot, treating it with a solvent. The separation of fullerenes from each other and their deep purification are also performed by means of solvents, using liquid chromatography methods [12]. These methods are based on the difference in the solubility of fullerenes of different types, and also on the difference in the sorption ability of fullerenes of different types in relation to some sorbents. The development of the above-described approach to the production of pure fullerenes in macroscopic quantities has provided researchers with the possibility of studying not only molecular properties of these compounds, but also crystal structures, optical, electrical, and others physical and chemical characteristics of fullerene as a bulk material.

Electric arc synthesis of fullerenes combined with subsequent chromatographic separation and purification have turned out to be quite effective means for production of endohedral fullerenes in macroscopic quantities. This has been made possible due to further development of the electric arc method using a graphite electrode with a hole filled with a mixture of metallic and graphite powders [13]. The studies addressed to the measurement and evaluation of the physical and chemical characteristics of endohedral compounds have been enhanced to a new stage as a result of this innovation. The possibility of synthesis of these compounds in macroscopic quantities allows the use of such effective analytical methods as optical, electron, NMR, EPR and Raman spectroscopy, electron and X-ray diffractometry etc. in their investigation. As a consequence, not only the fact of existence of a large family of chemically stable endohedral compounds has been stated with a high degree of reliability, but also the peculiarities of their structure as well as their electrical, optical and mechanical characteristics have been determined. This permits us to consider endohedral fullerenes as a new wide class of molecular nanostructures with promising prospects of scientific and practical applications.

A considerable volume of information about endohedral fullerene compounds has been accumulated. The list of elements whose atoms have been encapsulated inside a fullerene cage involves a noticeable part of the Periodic Table. Unique data about the charge state of these atoms, their exact geometrical position, and the character of vibrational movement inside the fullerene cage, as well as about features of chemical bond between encapsulated atom and carbon atoms in a fullerene molecule have been obtained. Besides that, data related to properties of endohedral fullerenes in the crystalline state (fullerites) have been obtained. In particular, it has been stated [14] that some endohedral metal fullerene molecules, due to the considerable off-center displacement of an encapsulated metal atom, are characterized by a quite large permanent dipole moment, which determines the character of intermolecular interaction in a crystal. This in turn causes an ordered arrangement of endohedral molecules in a crystal, providing these crystals with spontaneous electrical polarizability and ferroelectrical properties as a consequence.

The electronic structure of most endohedral metal fullerenes is determined by the phenomenon of transfer of all or part of the valence electrons of the encapsulated metal atom onto the outer surface of the fullerene molecule, thereby filling the existing electron vacancies [15]. This provides endohedral fullerene molecules with specific chemical properties different from those of both hollow fullerene molecules and separate metal atoms. The occurrence of some quantity of weakly bound electrons on the outer surface of an endohedral fullerene molecule provides this molecule with a strong reducing ability and offers a possibility for its participation in various chemical reactions resulting in adding various atoms, molecules or radicals. This considerably broadens the class of objects under investigation. Thus, the chemistry of endohedral compounds can be considered as a new branch of chemical research. In this point one should note an interesting peculiarity of endohedral chemical compounds. Indeed, an encapsulated particle (atom or molecule) undergoes off-centered displacement inside a fullerene molecule. This causes an additional asymmetry of the fullerene molecule, so that chemical compounds formed in consequence of joining some radical to a fullerene molecule at various points of its surface, should differ from each other in their properties. This kind of the chemical isomerism is not

observable in the case of 'hollow' fullerenes containing no atomic particles. The investigation of distinctions in the physical and chemical properties of isomers of endohedral compounds comprises a new direction in regiochemistry [16].

This article contains a review of studies in the field of endohedral fullerenes. Methods of synthesis of endohedral molecules and techniques of investigation of their physical and chemical properties are considered. Results of such investigations and prospects of further development of this branch of the chemical physics are analyzed. Some earlier advances in the field of production and investigation of endohedral compounds were considered in detail in the review articles [15].

2. Methods for production and purification of endohedral fullerenes

In general, an endohedral molecule can be synthesized in two ways. The first is to provide conditions of synthesis such that some portion of synthesized molecules turn out to be filled with atoms or molecules. In so doing, the conventional graphite with an addition of a finely dispersed powder of an encapsulated element is used as an initial material for endohedral compound production. Thermal sputtering of graphite under the action of an outer energy source is accompanied by atomization of the admixed material. This promotes the subsequent endohedral fullerene formation. The second way for synthesis of endohedral compounds is based on the incorporation of atoms or molecules inside already prepared fullerene molecules. If the substance of atoms or molecules to be encapsulated is normally in the gas state, such an incorporation can be performed by just keeping the fullerenes in an atmosphere of this gas under enhanced temperature and pressure. The heating promotes opening 'windows' in a fullerene molecule and the enhanced pressure simplifies the penetration of particles into the cage. As for the incorporation of atoms of normally condensed substances, this is reached through the irradiation of a fullerene crystal or film with atoms or ions accelerated to an energy sufficient for the penetration of a particle into the cage.

2.1 Laser sputtering

This method of synthesis of fullerenes was used in the pioneering work [1] resulted in their discovery. According to this method, a graphite disk is treated with laser irradiation of moderate intensity. A double-frequency Nd-YAG laser ($\lambda = 532$ nm) with a pulse duration of 5 ns and energy of 30–40 mJ was used as the source of irradiation. A carbon vapor stream formed as a result of graphite vaporization is entrained with a helium flow to be condensated with the formation of clusters containing a rather low yield of fullerenes.

In order to obtain endohedral fullerenes, some quantity of the vapor of the element to be incorporated into the fullerene cage must present in the high temperature region. In the first experiments [11] it was reached by using a specially prepared low density graphite impregnated with an aqueous solution of $LaCl_3$ as the target. The graphite surface was irradiated by focused laser pulses of wavelength 532 nm, duration 5 ns and energy 30–40 mJ. After termination of the laser pulse, the irradiated surface was blown with a helium flow emitted by a pulsed nozzle. The carbon vapor with an admixture of lanthanum vapor was swept away by the helium flow. The cooling of carbon atoms was followed by their condensation and the formation of carbon clusters. The cluster beam obtained was directed to the mass-spectrometer chamber. The mass spectrum of clusters formed as a result of the thermal sputtering of the target material is shown in Fig. 1. As is seen, it contains, apart from conventional hollow fullerenes C_{60}, C_{70} etc., the endohedral fullerenes $La@C_{60}$ and $La_2@C_{60}$.

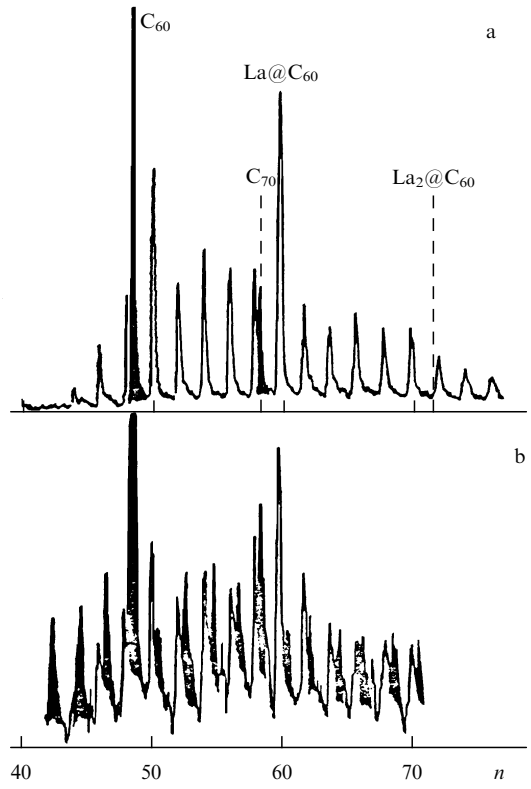

Figure 1. Mass spectra of carbon clusters obtained as a result of laser vaporization of the graphite disk surface [11]: (a) intensity of ionizing ArF laser irradiation is 1–2 mJ cm^{-2}; (b) < 0.01 mJ cm^{-2}.

The synthesis of endohedral fullerenes in macroscopic quantities was first performed in Ref. [13], as an important peculiarity of which the use of a composite laser target should be noted. The target was manufactured by pressing a mixture of La_2O_3, graphite powder, and pitch. It was placed into a heated cylindrical chamber filled with helium. As follows from the mass-spectrometric data, laser irradiation of the metal-containing graphite material in a helium atmosphere results in the formation of both conventional fullerene molecules and endohedral fullerenes of the type $La@C_{2n}$, where $2n = 60$, 70, 74 and 82. The toluene extract obtained from this soot contained only $La@C_{82}$.

The laser method of vaporization of a metal-containing graphite was developed further in Ref. [17], where a large number of endohedral actinide-containing compounds including uranium compounds $U_m@C_{2n}$, $U@C_{28}$, $U_2@C_{60}$ and also compounds of metals belonging to the main groups were produced. Using X-ray photoelectron spectroscopy, it has been shown that uranium atoms in the endohedral fullerene compounds $U@C_{2n}$ are chemically inert and have formal valence 4^+.

The method of synthesis of endohedral fullerenes based on laser action on composite material targets has not received

subsequent wide acceptance, which is caused mainly by rather low productivity and low yield of fullerenes inherent to this method. However, a few situations are known where the use of the laser vaporization method allows the production of some endohedral compounds which cannot be produced using the much more widespread electrical arc method. The above-mentioned endohedral uranium compounds synthesized in Ref. [17] belong to this set.

2.2 Electric arc method

The electric arc method is characterized by considerably higher parameters. This most widespread method is based on the use of the standard procedure of fullerene production, which was developed first by Krätchmer and Huffman [5]. In this procedure, the thermal sputtering of a graphite electrode in an electric arc burning in a helium atmosphere results in the formation of a soot containing up to 20% fullerenes, mainly C_{60} and C_{70}. The fullerenes are produced as a result of condensation of a carbon vapor, the formation of which follows the thermal sputtering of an anode material in a high temperature (above 3000 K) region of the electric arc. Adding some small quantity of metal vapor results in the formation of endohedral metal fullerenes in the same region, whose content in total fullerene substance contained in the soot does not exceed several percent.

The most simple way for inserting a metal vapor into an arc is based on the use of a composite electrode (anode) which consists of graphite with some admixture of a powdered metal or a compound of it (oxide, carbide). This method was first applied in Ref. [18], where a rod manufactured by compressing and subsequent annealing of a mixture of graphite powder, La_2O_3 and dextrine as a binder was used as an electrode. The further modification of this approach [19–21] resulted in a significant simplification of the anode manufacturing procedure. The use of a graphite rod with a hole drilled from the edge side and filled with a mixture of amorphous finely dispersed graphite and powdered metal or an oxide or carbide turned out to be appropriate. The typical content of metal in the anode material does not exceed several percent. The procedure of manufacturing the graphite anode with a drilled hole is described in detail particularly in Ref. [22], where such rods were used for synthesis of soot containing endohedral fullerenes of type $M@C_{82}$ (M = Sc, Y, La). In doing so, it has been stated that the yield of endohedrals is increased either due to inserting metal carbides into an electrode material or if the carbide-rich cathode deposit formed during the arc-driven vaporization of the metal-containing graphite rod is afterburned periodically through the change in polarity of electrodes.

As an example of effective usage of the electric arc method for production of endohedral fullerenes-containing soot, Ref. [23] can be mentioned, where the endohedral lanthanum fullerene compound $La@C_{82}$ in a pure form was first produced in a macroscopic quantity. The anode was manufactured by drilling a hole 270 mm in length and 10 mm in diameter in a graphite rod 300 mm in length and 15 mm in diameter. This hole was filled with a mixture of powdered graphite and La_2O_3. The content of La in the anode material amounted to 1.6 at.%. The rods were strengthened through keeping in an oven at 100 °C for 30 h followed by slow (at a rate of 30 K h^{-1}) heating to 900 °C and subsequent holding at this temperature in an argon flow. The rods were repeatedly treated at 950 °C in a vacuum of 10^{-5} Torr for 30 h in order to remove organic contamination and lower the oxygen concentration in the material. Since thereafter the rods became hygroscopic and sensitive to the wet, it was necessary to use them as soon as possible in order to obtain the maximum yield of endohedral metal fullerenes. A rod from pure graphite was used as the cathode. The arc was burnt in an atmosphere of flowing helium at a pressure of 500 mbar and a current of 250 A. The soot was entrained with a helium flow passing a filter under oxygen-free conditions. Fullerenes were extracted from the soot with the use of hot toluene or CS_2 over 24 h. A similar procedure was also used in Ref. [24] aimed at the synthesis and purification of endohedral molecules $Sc_3@C_{82}$. The fullerene-containing soot was produced in the arc discharge with graphite electrodes which were manufactured by vacuum sintering of the mixture of Sc_2O_3 (2.5 g) with graphite powder (4.3 g) for 5 h at $T = 1000$ °C followed by holding for 5 h at 1600 °C. The arc was burnt at a He pressure of 50–100 Torr and current of 500 A.

The above-described procedure of production of fullerene-containing soot was used first in 1990 and has reached the present time without any serious changes. The most considerable modification of this procedure is related to the rather high sensitivity of endohedral metal fullerene production to the presence of oxygen of air. Providing oxygen-free conditions results in a noticeable increase in the endohedral metal fullerene yield and the concentration of molecules incorporating several metal atoms. This effect was first discovered in Ref. [25], where endohedral metal fullerenes of type $M@C_{82}$ (M = Sc, Y, La) were produced. A setup isolated from the air was built to overcome this problem.

The technical problems related to the necessity of sealing the setup to provide "anaerobic" conditions were resolved more simply in Ref. [26], by filling the chamber with a buffer gas at atmospheric pressure. The fullerene-containing soot obtained in such a manner can be kept some time in the open air while their pores are still filled with an inert gas.

One more modification of the electric-arc method for production of a fullerene-containing soot concerns complicating the chemical composition of the rod. Thus, in Ref. [26] devoted to the synthesis and investigation of endohedral fullerenes $M@C_{82}$ (M = La, Y, Ce, Gd), graphite rods 15 mm in diameter containing 1 wt. % boron nitride along with a metal oxide (the content of metal comprised 1.5 at.%) were used. The thermally treated rods underwent arc-discharge thermal sputtering at a current of 350 A and He pressure of 100 mbar. As follows from measurements, the addition of boron nitride results in a 1.5–2 times increase of yield of both higher fullerenes and endohedrals.

A distinctive feature of the electric-arc method of production of fullerene-containing soot is the extraordinarily rich content of fullerene molecules of various kinds in the soot. This variety is broadened even more by being supplemented by endohedral fullerenes due to the addition of some quantity of a metal. The riches of the spectrum of fullerenes formed in a graphite-electrode arc-discharge plasma can be illustrated by the results of mass-spectrometric measurements performed in Ref. [21]. The content of soluble extract of the soot obtained through electric-arc sputtering of the graphite rod filled with either powdered lanthanum or lanthanum oxide La_2O_3 was investigated. The metal content in the rod material ranged between 0.5 and 5 at.%. The arc was burnt in an He atmosphere (180–220 Torr) at a current of 95–115 A and voltage of 20–25 V. The rise in the metal content in the electrode material was followed by an increase in the fraction of $La_2@C_{72}$ relative to other endohedrals. The mass spectrum

of extract from the soot obtained using a laser desorption time-of-flight mass spectrometer is shown in Fig. 2. The extraordinary richness of the spectrum containing both hollow fullerenes C_n, $n = 74, 76, 78, 80, 84, 84, 86, \ldots, 104$, and endohedrals $La_m@C_n$ ($m = 1, 2$; $n = 72, 74, 76, 78, 80, 82$) is noteworthy. One can also noted the absence of fullerene C_{72}, while the endohedral compound $La_2@C_{72}$ is present. This shows that a metal atom incorporated into the fullerene cage enhances its stability. The mechanism and features of this effect will be considered in detail below.

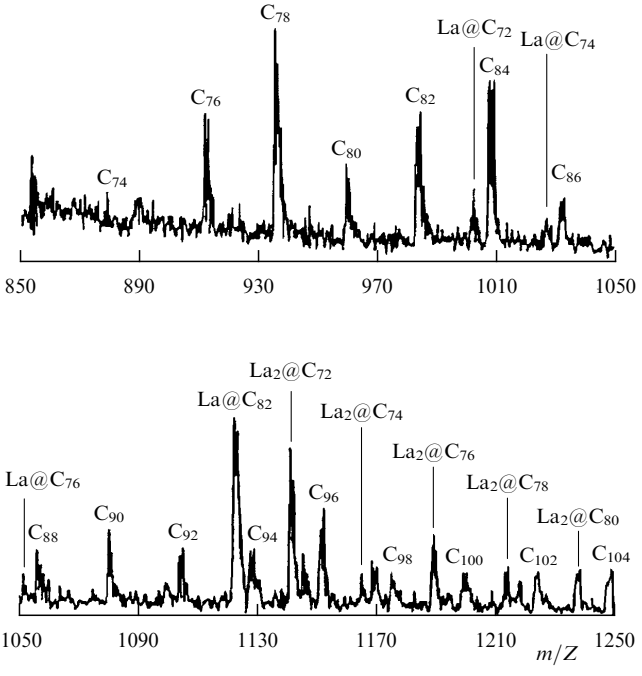

Figure 2. Laser desorption time-of-flight mass spectrum of the soluble extract of the soot formed by electrical arc sputtering of a graphite rod the inner hole of which is filled with a mixture of powdered La_2O_3 and amorphous carbon [21].

One more modification of the electric-arc method for the production of endohedral fullerenes consists in the substitution of metal powder with a gaseous metal carrier added into the electrical discharge chamber in parallel with a buffer gas flow. This method was used in particular in Ref. [27], where the endohedral fullerene $Fe@C_{60}$ was produced by graphite electrode arc burning in an atmosphere of $He + Fe(CO)_5$. Using the electric-arc method, the majority of known metal-containing endohedral compounds was produced, among which are those containing rare-earth metal atoms (La, Y, Sc, etc.).

The important parameter determining the effectiveness of synthesis of endohedral fullerenes in an electric arc is the temperature in the region of burning. Since the size of this region in a dc arc used for fullerene synthesis is usually much less than that of an electric-arc chamber, this arc is characterized by a considerable temperature nonuniformity. Under these conditions the gravity forces and a difference in the gas density in regions of different temperature cause free convection which lowers the gas temperature near the interelectrode gap. This in turn lowers the effectiveness of fullerene synthesis. An interesting way to overcome the free convection was proposed and realized in Refs [28 – 30], where the fullerenes were produced in a pulsed arc discharge with suppressed gravity. To this end, a tower 12 m in height and 2×2 m in base was built of tubes 4.85 cm in diameter. The arc is burnt in a cylindrical chamber 11 cm in diameter and 18 cm in height equipped with a graphite anode 10 cm in diameter and 100 mm in length and a graphite cathode 10 mm in diameter. The chamber was suspended inside the tower on a rope and repeatedly underwent the free fall for 1.1 s. The powdered La_2O_3 (9.3 wt.%) was impressed into the anode rod. The discharge burnt at an He pressure of 300 Torr, an interelectrode gap of 5 mm, a current of 20 – 40 A, and voltage of 20 – 30 V. The discharge current was synchronized with the chamber oscillations and flowed only during its free fall. As shown by calculations, a temperature sufficient for the synthesis of fullerenes is reached in 0.01 s, which is much shorter than the free-fall time, so the fullerenes are surely synthesized under the free-fall conditions. The measurements indicate that the soot production under the suppressed gravity twice exceeds that reached in the presence of gravity. According to estimates performed, the production of LaC_{82} (endohedral structure not confirmed) under the non-gravitational conditions exceeds that for conventional conditions by about 14 times. Under these conditions the excess in production of C_{60} may be as great as 2.5 times.

2.3 Gaseous method of synthesis of endohedral fullerenes

Hollow fullerene molecules synthesized by conventional methods can absorb gaseous atoms or molecules, forming endohedrals [31], as a result of long-time heating at an enhanced gas pressure. This method was used for synthesis and investigation of endohedral molecules containing rare-gas atoms He, Ne, Ar, Kr, Xe [31 – 39] and simple molecules (CO [40], CN [41]).

As the detailed investigations performed, in particular, in the above-cited works showed, keeping fullerenes in a gas atmosphere at an enhanced pressure and temperature for a long time results in the establishment of a thermodynamic equilibrium between hollow and endohedral fullerene molecules. The optimal conditions depend on the type of gas and lie in the temperature range of 600 – 1000 °C and gas pressure of several thousand atmospheres. The optimal equilibrium content of endohedral molecules does not exceed one tenth of a percent. Subsequent enrichment of a material by standard chromatographic methods permits obtaining endohedral molecules in a quantity sufficient for investigation of not only the structure but also the physical and chemical characteristics.

It is interesting to note that the use of the gaseous method provides the synthesis of endohedral molecules containing not only one but also two rare-gas atoms. Thus, endohedrals $^3He@C_{70}$ and $^3He_2@C_{70}$ were synthesized in Ref. [32] by keeping 200 mg of C_{70} of 96% purity in a copper tube at a ^3He pressure of 3000 atm and temperature of 650 °C for 8 h. As is shown by NMR and mass-spectroscopic measurements, the ratio of the components C_{70}, $^3He@C_{70}$, and $^3He_2@C_{70}$ in the sample is approximately 37:1:0.05.

2.4 Ion implantation

One more quite effective method for endohedral fullerene production is based on the irradiation of hollow fullerenes with ions of the element to be incorporated into the fullerene cage. This method has manifested itself as irreplaceable in producing endohedral compounds containing atoms of elements of enhanced chemical reactivity. Thus, the authors

of Refs [42 – 49] succeeded in the synthesis of the compound $N@C_{60}$ using this method. In doing so, the very high chemical activity of atomic nitrogen, having unpaired valence electrons, was almost fully suppressed.

This compound was produced by irradiating a fullerene film, deposited on a substrate, with nitrogen ions. A standard ion emitter or a glow discharge were used as the source of nitrogen ions. There are two experimental setups corresponding to these methods. In the first (Fig. 3), a film of C_{60} is deposited on a copper substrate and simultaneously irradiated with nitrogen ions emitted by a plasma source. The ion energy is controlled by varying the voltage between the source and the target. Typical magnitudes of the energy and current of ions accounted 40 eV and 50 μA, respectively. The ratio of ion currents $N_2^+ : N^+$ was about 7:1. After several hours of deposition the film thickness reached 2 – 4 μm. Then the deposit was removed from the copper substrate, dissolved in toluene, and filtered. The soluble fraction usually comprised 10 – 20%, whereas the rest of the material was left on the filter. This soluble fraction (1 – 2 mg), which was C_{60} with an admixture of $N@C_{60}$ ($10^{-4} - 10^{-5}$) was studied by EPR spectroscopy.

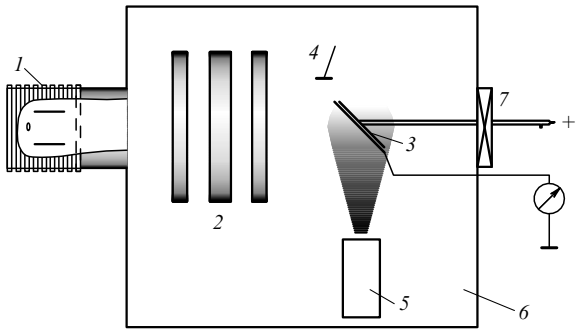

Figure 3. An apparatus for the production of $N@C_{60}$ through the simultaneous deposition of C_{60} on a substrate and irradiation of the substrate with nitrogen ions [43] (schematic): *1*, nitrogen ion source; *2*, electrostatic lens; *3*, substrate for fullerene deposition; *4*, device controlling the thickness of the coating; *5*, fullerene beam source; *6*, vacuum chamber; and *7*, water cooling.

The second method for production of endohedrals $N@C_{60}$, based on the use of a glow discharge, is much simpler in realization and can be used in any laboratory. However, it has not yet been optimized. The experimental setup (Fig. 4) involves a quartz tube with two electrodes through which a nitrogen flow is passed. The central part of the tube, in which C_{60} is deposited, is surrounded by a furnace. C_{60} is sublimed on the water-cooled cathode during the action of the discharge current. After several hours of discharge burning, a deposit 10 – 50 mg in mass containing, apart from C_{60}, also $N@C_{60}$ in a concentration of $10^{-6} - 10^{-5}$ is formed. The content of endohedral molecules in the fullerene substance when the gas-discharge method of their production is applied is several times lower in comparison with that for an ion source. However, the former seems to be preferable due to its simplicity, higher productivity (in relation to the mass of the deposit produced) and unrealized possibilities of improvement.

The ion-implantation method seems to be even more effective in the production of endohedral compounds containing alkali metal atoms [50 – 54]. The use of standard

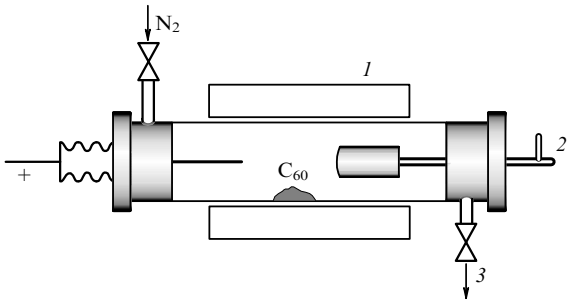

Figure 4. An apparatus for the production of $N@C_{60}$ through ion implantation in a gas discharge chamber (schematic): *1*, furnace, *2*, water cooling device; *3*, to pump.

electric arc methods for this aim meets severe technical difficulties related to the high chemical reactivity of alkali metal atoms. Therefore, the ion-implantation method seems to be the only possible way for producing such compounds. In this method, described in detail in Refs [50 – 54], a film of pure fullerene C_{60} or C_{70} is deposited on a silicon or nickel disk substrate 2.5 cm in diameter at a temperature of 500 °C. The thickness of the fullerene film reached 30 monolayers. The film is irradiated with alkali metal ions after deposition of each monolayer. The energy of the ion beam is varied in the range 15 – 70 eV and is characterized by a spread of 1 eV. After termination of the deposition procedure the film is heated to 800 °C at a rate of 10 K s^{-1} in a high vacuum (about 10^{-9} Torr) for the desorption. Desorbed molecules are ionized by electron impact (the electron energy is about 70 eV) and detected in a quadrupole mass spectrometer.

Measurements show that the maximum yield of endohedral metal fullerenes $M@C_{60}$ and $M@C_{70}$, where M = Li, Na, K, Rb, is reached in the case of lithium and at a lithium ion energy of 30 eV and the ratio of the number of ions to that of target molecules 6 : 1 is about 50%. The rise in the alkali metal atom mass number results in a decrease in the yield, but the latter is never less than several percent. The ion beam energy dependence of the ratio of the endohedral signal to that of hollow fullerenes is shown in Fig. 5. As is seen, this dependence has a clearly pronounced maximum at some ion energy, which shows the existence of an 'energy window' for endohedral fullerene formation. The rise in the ion radius results in a displacement of the window in the direction of increasing energy. The existence of an optimal energy for endohedral fullerene formation is easily explainable on the basis of simple physical considerations. Low-energy ions cannot overcome an energy barrier preventing their penetration into the fullerene cage. At very high energy the collision of an ion with a fullerene molecule causes its decomposition. A rise in the ion radius causes a rise in the energy necessary for penetration of an ion into the cage. That is why the maximum is displaced in the direction of increasing energy, and the yield of endohedral fullerenes is lowered.

The investigations performed in Refs [50 – 54] have shown that endohedrals are not usually destroyed as a result of impact ionization at electron energy 70 eV. A signal related to endohedrals containing two encapsulated lithium atoms is observed in mass spectra. The intensity of this signal is about six times lower than that for endohedrals with one encapsulated atom. The binding energy of hollow and endohedral fullerene molecules in the film was estimated using the temperature dependence of the thermal desorption signal.

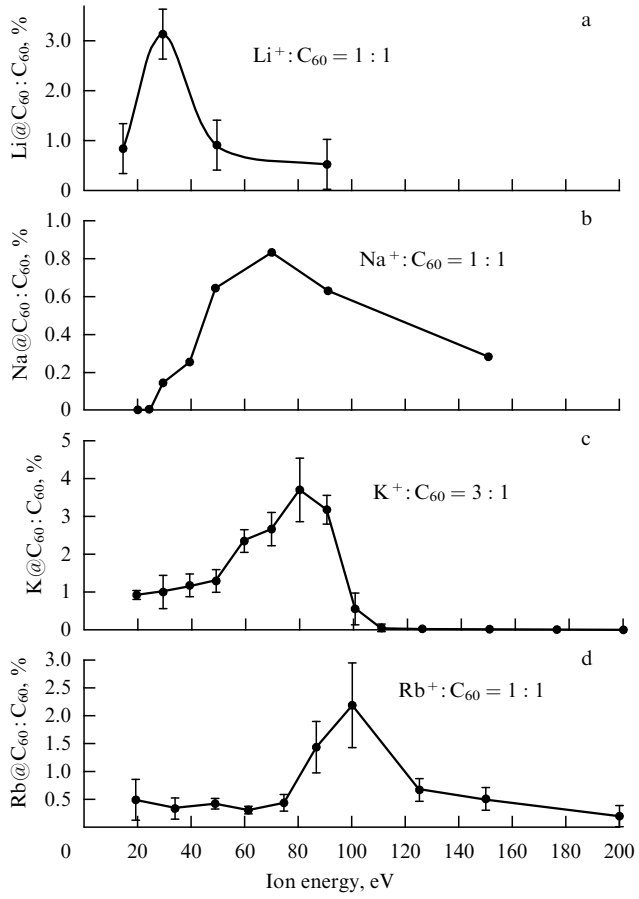

Figure 5. Dependence of the ratio of endohedral fullerenes to that of hollow fullerenes on the energy of ions used in irradiation of the fullerene film [50].

For pure fullerene it is 137 ± 4 kJ/mol, while the rise in the content of endohedrals results in increasing this quantity.

The mechanism of trapping of an atom as a result of the collision with a fullerene cage was studied in detail in Ref. [51], where the energy dependences of the cross section of capture of He and Ne atoms with the charged molecule C_{60}^+ were measured and calculated. The results of this work show two different mechanisms of capture of the He atom by a fullerene cage. By the first mechanism, the He atom penetrates through a six-member ring without any notable damage in the fullerene molecule. This mechanism is characterized by a threshold collision energy of about 6 eV and a maximum cross section close to 8×10^{-17} cm^2. The second mechanism can be interpreted as a result of scattering of the He atom on a C_2 fragment entering into the fullerene cage. Under favorable conditions this can result in an additional opening of the cage, which promotes the penetration of the scattered atom into the cage. This mechanism is characterized by a threshold collision energy of about 11 eV and a sharper rise in the cross section with a rise in the collision energy. The maximum cross section value is reached at about 20 eV and measures about 4×10^{-16} cm^2. A further rise in the collision energy results in the predominant decomposition of the fullerene molecule.

The above-outlined concepts of the mechanisms of penetration of a fast atom into a fullerene cage seem to be inapplicable for the case of incorporation of the Ne atom, whose characteristic size is about 1.5 as large as that for He. In this case the penetration of an atom into the fullerene cage is possible only if the fullerene molecule is in a vibrationally excited state. The vibrations of carbon atoms in the molecule cause a periodical increase in the six-member ring size, which promotes the penetration of the Ne atom into the fullerene cage during the collision. The characteristic vibration energy sufficient for the penetration of the Ne atom into the fullerene cage is estimated as 20–30 eV, while the threshold collision energy is 18 eV. It should be noted that the penetration of the Ne atom into the fullerene cage results in a local break of a bond, which is restored with some probability after the collision.

2.5 Others methods of synthesis of endohedral fullerenes

There are also other methods for the solution of this task along with the above-described ones. The realization of these methods requires special equipment, for which reason these methods are not widespread as the above-described ones. However, these methods can in some relations be even more effective than conventional ones and can give qualitatively new results which are unattainable using other methods. Thus, the authors of Ref. [56] produced endohedral metal fullerenes by vaporizing a mixture of soot with metal oxides using a plasma torch. The yield of hollow fullerenes and endohedral metal fullerenes $Y_2@C_{80,\,82}$ turned out in this case to be comparable with that attained using an arc discharge.

The methods of synthesis of endohedral fullerenes based on the use of nuclear transmutation reactions look even more exotic. Thus, the fullerene $Be@C_{60}$ was produced as a result of penetration of a fast recoiling nucleus ^{7}Be, formed via a nuclear reaction, inside the fullerene cage [57]. The nuclei ^{7}Be with a half-life of 53.3 days were produced using two nuclear reactions: ^{7}Li(p, n)^{7}Be and ^{12}C(γ, αn)^{7}Be. Their γ decay (energy 478 keV) results in the formation of ^{7}Li. In the case of the reaction ^{7}Li(p, n)^{7}Be, 10 mg of fullerene C_{60} of 99.5% purity was mixed with powdered Li_2CO_3 in the weight ratio 1:1. Then the mixture was wrapped into an aluminum foil and irradiated with protons at an energy of 12 MeV and current 2 μA for 2 h. In the case of the reaction ^{12}C(γ, αn)^{7}Be, 10 mg of C_{60} of 99.5% purity was also wrapped into an aluminum foil. Then the sample was placed inside a quartz tube and irradiated with γ quanta with an energy of 50 MeV for 12 h. The bremsstrahlung formed upon scattering of an accelerator-driven electron beam of energy 300 MeV and current 120 μA on a platinum target was used as a source of γ quanta.

In both cases the irradiated samples were dissolved in CS_2, filtered and then, after evaporating the solvent, were subjected to the separation procedure in a Buckyclutcher HPLC facility using a toluene–hexane mixture in the ratio 7:3 as an eluent. The shape of the chromatogram, supported by the measurements of the time dependence of γ-radiation intensity, shows the practically full separation of endohedral and hollow fullerenes.

The radiation method for production of endohedral fullerenes was developed further in [58–60], where rare-gas atoms were used as the recoiling nuclei. Ref. [58] deserves a more detailed consideration. In this work the incorporation of xenon and krypton atoms inside the fullerene cage resulted from recoiling in the deuteron-stimulated nuclear reactions ^{127}I(d, 2n)^{127}Xe and ^{79}Br(d, 2n)^{79}Kr. The recoiling xenon and krypton nuclei have an energy of several hundred eV, which permits them to penetrate the fullerene cage. The radioactive nuclei of ^{127}Xe (^{79}Br) formed again undergo a decay, resulting in the (formation) of ^{127}I (^{79}Br) having a half-life of 36.4 days (34.9 h), followed by the emission of characteristic γ quanta

with an energy of several hundred keV. Four samples were prepared by homogeneously mixing 10 mg of C_{60} (C_{70}) with 10 mg of KI (KBr), and one sample was prepared by mixing 10 mg of a mixture of $C_{60} + C_{70}$ with 10 mg of KI. The samples were irradiated for one hour with 16-MeV deuterons from a cyclotron source (5-μA current). The irradiated sample was dissolved in *o*-dichlorobenzene, which was followed by the chromatographic procedure. The samples produced were controlled using a γ-quantum detector. The characteristic emission of radionuclides was convincing evidence of the endohedral nature of the compounds synthesized. The total quantity of endohedral fullerenes Xe@C_{60} and Kr@C_{60} was estimated as about 10^{10}. The occurrence of fullerene dimers and trimers (one of which was endohedral) was noted in the solution. It was supposed that such clusters were formed as a result of an impact during the penetration of a radionuclide into the fullerene cage.

A higher yield of endohedral fullerenes was observed in Refs [59, 60], where a crystalline fullerene C_{60} with rare-gas atoms intercalated inside the lattice was used as the initial material. This resulted in the formation of endohedral fullerenes with radionuclides of rare gases, encapsulated in the fullerene cage. Samples of C_{60} were subjected to an enhanced rare gas pressure (about 1700 atm) at a high temperature, which caused the intercalation of rare-gas atoms into the fullerene crystal lattice with the stoichiometry Ar_1C_{60}, $Kr_{0.9}C_{60}$ and $Xe_{0.4}C_{60}$. The obtained samples 0.4 g in weight were irradiated with a neutron flux of $5 \times 10^{13}\,\mathrm{cm^{-2}\,s^{-1}}$ in a reactor for 4 h. Then the crystal fullerene samples as well as their solutions were subjected to gamma-spectroscopic investigations. As follows from the X-ray diffraction measurements, the neutron irradiation of fullerene crystals did not notably change their crystal lattice. The fact of endohedral fullerene formation as a result of neutron irradiation followed by the gamma emission of atoms was indicated by the activity of fullerene solutions after neutron irradiation of the crystal. The number of endohedrals was estimated as 1–2 % of the activated rare-gas atoms.

Nuclear methods are used not only for obtaining fast particles capable of penetrating the hollow fullerene cage, but also for changing the sort of an atom, already encapsulated inside such a cage. This permits the production of endohedral fullerenes that can hardly be synthesized using conventional methods. Besides that, the endohedral fullerenes containing atoms with radioactive unstable nuclei are detectable quite easily using appropriate apparatus, which facilitates the investigation of the behavior of such systems. Such a transformation was performed first in [61], where the crystal Gd@C_{82} produced by the conventional electric-arc method was acted on by thermal neutron irradiation. This irradiation stimulated the β decay of nuclei followed by the nuclear transformations $^{161}\mathrm{Gd} \rightarrow {}^{161}\mathrm{Tb} \rightarrow {}^{161}\mathrm{Dy}$. It was found that the nuclear transformations do not violate the stability of endohedral compounds.

The above-described approach was further developed in a recent work [62] devoted to a comparative study of stability of endohedral fullerenes with encapsulated metal atoms of various types. Pure samples of endohedral fullerenes Sm@C_{82} and Yb@C_{82} produced via the standard arc-discharge procedure followed by chromatographic purification were used as initial substances. The samples were irradiated with a thermal neutron flow at a density of about 10^{12}–$10^{13}\ \mathrm{cm^{-2}\,s^{-1}}$. The neutron activation of Sm nuclei encapsulated in a cage resulted in a series of nuclear transformations $^{155}\mathrm{Sm} \rightarrow {}^{155}\mathrm{Eu} \rightarrow \mathrm{Gd}^{155}$. After irradiation, the chromatographic separation and purification procedure was repeated again. It was observed that the nuclear transformation of metals practically does not violate the endohedral fullerene stability. In a similar way, microcrystals of Yb@C_{82} were irradiated with a neutron flux of $2.8 \times 10^{13}\,\mathrm{cm^{-2}\,s^{-1}}$, which caused the decay reactions $^{177}\mathrm{Yb} \rightarrow {}^{177}\mathrm{Lu} \rightarrow {}^{177}\mathrm{Hf}$. However, in this case the nuclear transformation $^{177}\mathrm{Yb} \rightarrow {}^{177}\mathrm{Lu}$ resulted in a violation of the stability of the fullerene structure, so that the endohedral compound Lu@C_{82} was practically not observed. Such a difference in the stability of fullerenes formed as a result of nuclear transformations can be explained taking into consideration the change in the oxidation state of an atom formed (oxidation state of Yb is +2, while that of Lu is +3). Thus, a rearrangement of the electronic structure of endohedral fullerene as a consequence of a change in the oxidation state of an encapsulated atom can violate the stability of the former.

One more publication should be mentioned [63], which concerns the investigation of the dynamic behavior of the cerium atom in the cage of the endohedral compound ^{140}Ce@C_{82}. This compound was synthesized by irradiating a sample of ^{139}La@C_{82} 3 mg in weight with a neutron flux of $10^{14}\ \mathrm{cm^{-2}\,s^{-1}}$ for 10 h. The neutron activation of the lanthanum nucleus caused the formation of the unstable nucleus ^{140}La followed by β^- decay and the formation of the nucleus ^{140}Ce. The obtained samples of ^{140}Ce@C_{82} were repeatedly purified from contamination formed in the course of irradiation using a chromatographic column and were prepared in the form of a powder and *o*-dichlorobenzene solution for further investigations.

2.6 Extraction and purification of endohedral fullerenes

The most frequently used method of extraction of fullerenes from a fullerene-containing soot [5, 12] is based on the fact that the fullerene is in essence the only carbon modification that is soluble in the majority of organic solvents such as toluene, benzene, xylene, etc. (The behavior of fullerenes in solutions is considered in detail in our recent review article [10], also containing a set of relevant reference data.) The soot is washed with one of these solvents, which results in the extraction of the fullerenes into a solution. Since the dissolving procedure is very slow, it is appropriate to provide continuous flow of the solvent through a soot. The solution obtained is evaporated continuously, and the condensed vapor of the solvent is passed again through the soot. Continuous vaporization of a solvent increases the concentration of the solution up to its saturation, which is followed by precipitation of a deposit in the form of a polycrystalline powder containing fullerenes of various types. The setup operating in the above-described manner is called SOXHLET and is used extensively for the extraction of fullerenes from soot.

A mixture of various types of fullerenes obtained as a result of extraction is separated into pure components using methods based on ideas of liquid chromatography. In doing so, a solution containing fullerene molecules of various types is passed through a sorbent, which is a porous material having a different sorption ability in relation to fullerene molecules of various types. Fullerene molecules contained in the solution are sorbed by the porous surface of a sorbent. The subsequent treatment of the sorbent with pure solvent results in the

extraction of fullerene molecules from the sorbent into the solution. The sorption abilities of a sorbent in relation to fullerene molecules of different types are generally different. Thereby, the characteristic time of desorption is a specific property of the molecule. The use of long columns filled with a sorbent permits the separation not only of fullerene molecules of different types, but also (in some cases) molecules differing in isomeric structure. The chromatographic procedure can be repeated many times in the case of necessity for further purification of fractions extracted. In doing so, the best results are reached using sorbents of different types in the various stages of the process.

The above-described principles of extraction, separation, and purification of fullerenes have received wide acceptance already at the initial stages of development of fullerene research [5, 12, 64, 65]. These principles, developed initially for separating hollow fullerenes, have also been used in the solution of the considerably more complicated problem of separation and purification of endohedral fullerenes. The main difficulty arising in the solution of this problem is the extraordinary low content of endohedral fullerenes in a fullerene-containing soot and relevant soluble extract. This difficulty can be overcome via the multiple repetition of the chromatographic procedure and using an appropriate combination of sorbents and solvents of various types at each stage of a process. The typical chromatograms observed for the sequential extraction of endohedral compound La@C_{82} [66] are shown in Fig. 6. As is seen, using the columns differing in the type of sorbent, in various successive stages of purification, fractions from the solution can be removed for which the retention time is close to that for the desired product La@C_{82}.

Since many of the endohedral fullerene molecules have a relatively high permanent dipole moment, they are solved quite readily in polar solvents. For this reason it is appropriate to perform the extraction procedure in two stages. The first one involves a nonpolar solvent (i.e., toluene) promoting the removal of the main mass of C_{60} and C_{70}. The second stage involves the mixture $CH_3OH + CS_2$ (in the ratio 16:84), containing the polar solvent. The content of endohedrals in the extract obtained reaches 0.1–0.5%. Various schemes of isolation of metal fullerenes used by various authors are given in Table 1. Using proper combinations of solvents, columns, and eluents at the first and second stages of the process, the

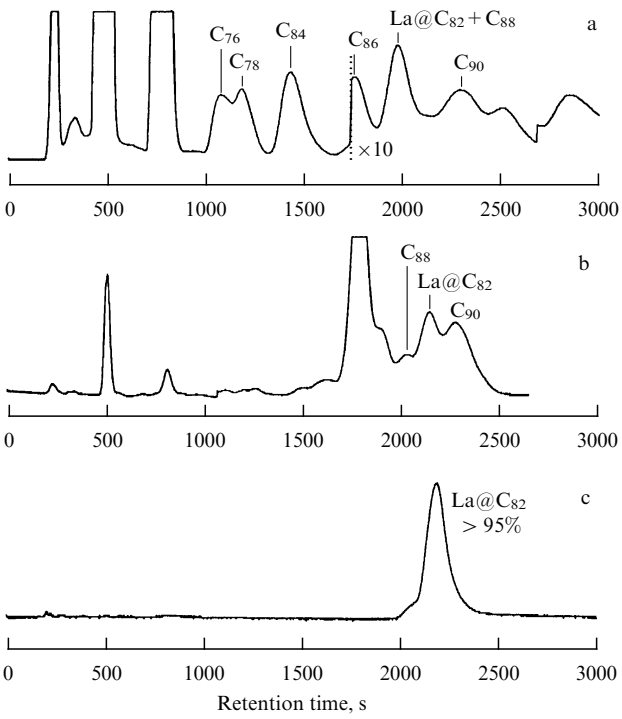

Figure 6. Chromatograms illustrating sequential chromatographic isolation and purification of the endohedral compound La@C_{82} [66]. Upper: chromatogram of the extract of soot produced using a graphite anode with the addition of La_2O_3 and Cosmosil as a separating column; middle: repeated chromatogram of the solution enriched in La@C_{82}, obtained using toluene as a solvent and the Buckyclutcher as a separating column; below: chromatogram of the solution enriched in La@C_{82} in the preceding stage, obtained using toluene as a solvent and the Buckyclutcher as a separating column.

Table 1. Schemes of separation and purification of endohedral fullerenes.

Endohedral compounds	Description of the column and eluent (the sorbent and solvent are indicated)	Method of extraction; solvent	Ref.
Sc_2@C_{74}, Sc_2@C_{82}, Sc_2@C_{84}	Two stages: (a) polystyrene/toluene, (b) Buckyclutcher (Trident-Tri-DNP); toluene/hexane (50:50)	SOXHLET; CS_2	[67]
La@C_{82}	Two stages: (a) Cosmosil (2-(1-pyrenil)-ethylsylitated silica); toluene, (b) Iteration of the stage (a)	SOXHLET; 1,2,4-trichlorobenzene	[68]
La@C_{82}	Two stages: (a) polystyrene/CS_2, (b) Buckyclutcher; toluene	SOXHLET; CS_2	[69]
Sc_3@C_{82}	Multiple-stage procedure Polystyrene/toluene; decaline	SOXHLET; CS_2	[70]
Pr@C_{82}	Two stages: (a) Cosmosil; toluene, (b) Buckyclutcher, toluene	SOXHLET; CS_2 or CS_2: methanol	[66, 71]
La@C_{82}	One stage: (*p*-carboxyphenyl) triphenyl-porphyrene (CPTPP)/silica gel; toluene:CS_2 (3:1)	(i) toluene; (ii) pyridine	[72–74]

authors of the cited works managed to produce samples of endohedral metal fullerenes in a quantity of up to 0.1 mg per day with a purity higher than 95%. The further development of the described methods of separation and purification of endohedral fullerenes resulted in a severalfold rise in the productivity of these methods, while the purity of samples obtained reached 99%. However, the procedure of obtaining endohedral fullerenes in a pure form remains rather laborious. Thus, as is shown in [26], the production of 10 mg of $M@C_{82}$ (M = La, Y, Ce, Gd) requires 40 – 50 chromatographic runs, which takes 25 – 35 h and consumes 30 – 40 liters of toluene.

An extension of the list of solvents used for the extraction of endohedral compounds from a fullerene-containing soot has resulted in a corresponding increase of the list of compounds synthesized. Thus, the use of aniline and pyridine [75, 76] for this aim permitted the extraction at relatively low temperatures of a variety of endohedral compounds including $Ca@C_{60}$, $Sr@C_{60}$, $Y@C_{60}$, $Ba@C_{60}$, $La@C_{60}$, $Ce@C_{60}$, $Pr@C_{60}$, $Nd@C_{60}$, and $Gd@C_{60}$. In doing so, providing anaerobic conditions was not necessary. In the works cited, a graphite anode was used, into which a powdered metal oxide (CaO, SrO, etc.) in contents of 0.3 or 0.8 mol. % was introduced. The arc was burnt at a current of 100 – 180 A, a voltage of 25 V and an He pressure of 100 – 200 Torr. Aniline or pyridine passed through the soot at $T = 273 - 278$ K for 3 – 5 h were used as a solvent. The extract obtained was studied via laser-desorption mass spectrometry. The mass spectrum of aniline extract contained peaks related to the above-mentioned endohedral compounds. The intensity of peaks was as a rule comparable with that of the hollow fullerenes C_{60} and C_{70}.

The procedure of isolation of various isomers of an endohedral fullerene compound seems to be even more complicated technically. Such molecules have equal masses but different spatial structure; therefore, the retention times inherent in their chromatograms are characterized by a very small difference. Besides that, the peaks of some isomers of endohedral compounds can be situated very closely to those of hollow fullerenes, which also hinders the isolation of isomers in a pure form. However, this problem can be successfully solved using a multiple-stage chromatographic procedure.

One of the first works devoted to the isolation of a specific structural isomer of an endohedral molecule in a pure form was performed in 1993 [69]. This work concerned the isolation of the major isomer of $La@C_{82}$ using two-stage liquid chromatography. The second, minor isomer of this compound was isolated in Ref. [77] by repeatedly using the one-stage chromatographic procedure. Due to the high sensitivity of this isomer to the presence of atmospheric air, each chromatographic run was followed by the outgassing of a solution.

The efforts of researchers, addressed to the isolation of isomers of endohedral molecules, became more well-directed after publication of the Atlas of Fullerenes [78], in which the systematic classification of fullerene isomers was introduced. The classification is based on the symmetry properties of fullerene molecules, determining their behavior under conditions of spectroscopic, NMR and EPR measurements. However, a so-called chromatographic classification based on the sequence of appearance of peaks related to corresponding isomers in the chromatogram is extensively used in parallel with the classification based on the symmetry properties of molecules [79]. In accordance with this classification, each isomer is labeled by the corresponding number I, II, III.., showing the position of the relevant peak in the chromatogram.

We now dwell in more detail on recently published works [80, 81] where all structural isomers (I – IV) of the endohedral molecule $Ca@C_{82}$ were first isolated and purified. A fullerene-containing soot was produced in an arc with electrodes fabricated from graphite with an about 0.3 at.% addition of a metal at a current of 350 – 400 A and an He pressure of 50 Torr under anaerobic conditions. The extraction of fullerenes from the soot was performed using CS_2 as an eluent. Endohedral molecules were isolated and purified up to 99.9% purity via two-stage chromatography using Cosmosil Buckyprep and Regis Buckyclutcher columns. In order to enhance the separating ability of the method, the two-stage separation procedure was repeated 2 – 9 times. The mass spectra of the extract contained all the endohedral molecules encapsulating a calcium atom, from $Ca@C_{72}$ to $Ca@C_{84}$, with a prevalence of molecules $Ca@C_{72}$, $Ca@C_{82}$ and $Ca@C_{84}$. Thus, endohedral molecules containing Ca differ notably in this regard from those containing lanthanides and Group IIIA metals, for which the prevalence of $M@C_{82}$ is inherent. In the separation of endohedral compounds $Ca@C_{82}$ and $Ca@C_{84}$ via two-stage chromatography, various isomers were obtained, labeled in accordance with the chromatographic classification as I, II, III, etc., in sequence of enhancement of the retention time. Four isomers of $Ca@C_{82}$ and two isomers of $Ca@C_{84}$ were obtained. All the isomers of $Ca@C_{82}$ were found on the tail of the fraction C_{84}, whereas the isomers of $Ca@C_{84}$ were found on the tail of the fraction C_{86}. Repeatedly using the two-stage HPLC separation procedure, each of the isomers can be purified up to 99%.

The above-described approach to the problem of producing, isolating, and purifying isomer modifications of metal-containing endohedral fullerene molecules was developed further in Ref. [82]. The endohedral compounds $Ca@C_{80}$, $Sr@C_{80}$, $Ba@C_{80}$, $Ca@C_{82}$, $Sr@C_{82}$, $Ba@C_{82}$, $Ca@C_{84}$, $Sr@C_{84}$ and $Ba@C_{84}$ were isolated in a pure form in macroscopic quantities and studied by optical spectroscopy and NMR. The fullerene-containing soot was produced via the standard method using graphite electrodes containing 0.3 at.% metal in the form of carbide. The arc discharge was burnt under fully anaerobic conditions at a dc current of 250 A and a voltage of 28 V. Helium was passed through the chamber at a flow rate of 12 l/min at a pressure of 40 – 70 Torr. The soluble fraction was extracted from the soot with CS_2 using sonication. Fullerenes were separated using a three-stage chromatographic procedure. At the first stage of separation, a Cosmosil 5PYE column was used, while the following stages were performed using a Buckyclutcher column. The analysis of chromatograms shows that this procedure provides the isolation of four isomers of $Ca@C_{82}$. The maximum abundance in the extract corresponds to isomer III. The abundance of isomers I and IV is twice lower, whereas that of isomer II is four times lower. Two isomers of fullerene $Ca@C_{84}$ situated on the slow shoulder of C_{86} were isolated. The amplitude of isomer I was nearly twice as large as that for isomer II and close to that for isomer III of $Ca@C_{82}$. A $Ca@C_{80}$ fullerene situated near the peak of C_{86} was also extracted in parallel with above-indicated endohedral fullerenes. This substance is separated readily from C_{86} and C_{84} using the Buckyclutcher column. Only one isomer of endohedral fullerenes $Sr@C_{82}$ and $Ba@C_{82}$ was observed.

The comparison of chromatograms obtained for various endohedral fullerenes $Ca@C_{84}$, $Sr@C_{84}$, $Ba@C_{84}$ shows that the rise in the atomic number of an encapsulated metal atom is accompanied by an enhancement in the retention time. However, this results in a decrease in the yield of the metal fullerene (down to 70% for Sr and to 20% for Ba) in comparison with that of isomer I of $Ca@C_{84}$. The authors ascribe such behavior to the rise in ionic radius as the atomic weight rises (0.099, 0.110 and 0.134 nm in the row calcium, strontium, and barium).

The procedure of chromatographic enrichment of endohedral fullerenes containing rare-gas atoms turned out to be most difficult for realization. This is caused by the chemical inertness of such atoms, due to which the sorption ability of endohedral fullerenes is very close to that of hollow ones. The gaseous method of production of endohedral fullerenes of this kind results in a very low content of these compounds in hollow fullerenes (no more than tenths of a percent). Therefore, this prevents the production of such molecules in a pure form in a macroscopic quantity. In this connection, it would be of interest to consider work [33], where the procedure of chromatographic enrichment of endohedral fullerenes $Kr@C_{60}$ in CS_2 solution using an alumina-based sorbent is described. The initial content of endohedral molecules in the sample of fullerene C_{60} amounted to about 0.1%. The separation procedure resulted in three fractions (slow, middle and fast) differing in the endohedral content. The endohedral content was analyzed by heating a sample for 2 h at 1000 °C followed by the measurement of the quantity of extracted xenon via a quadrupole mass spectrometer. The enrichment coefficient determined as the ratio of the contents of endohedral molecules in the slow and fast fractions ranged between 12 and 38%, depending on the type of solvent and sorbent. Such a low magnitude of the enrichment coefficient obviously makes the problem of producing pure samples rather complicated technically.

However, the authors of [35] managed to make a considerable advance in the solution of this problem. They demonstrated an effective chromatographic enrichment of $Ar@C_{60}$. Endohedrals were produced keeping the fullerene at a temperature of up to 1000 K and argon pressure of over 1000 atm for several hours. The resulting concentration of $Ar@C_{60}$ in the fullerene sample reached 0.1%. The enrichment of the substance in $Ar@C_{60}$ was performed by passing 0.5 ml toluene solution of the extract through a chromatograph equipped with a Cosmosyl column. The composition of the sample obtained was measured via a laser desorption mass spectrometer. The structure of endohedral molecules was studied by X-ray photoelectron spectroscopy (XPS). The concentration of $Ar@C_{60}$ in the enriched sample reached 40%. This corresponds to an enrichment coefficient of the chromatography procedure as large as 400.

3. The structure of endohedral fullerenes

The results of many experimental studies show a large variety of structures of endohedral fullerenes. Considering the structure of an endohedral compound, one can select two main questions relevant to this problem. The first concerns the structural peculiarities of a fullerene cage inside which one or several atoms of some element are incorporated. The second relates to peculiarities in the position of incorporated atoms inside the fullerene shell. Much information related to each of the two questions has been accumulated to date.

3.1 Magnetic resonance

The main source of such information is the measurements performed by the electron paramagnetic resonance (EPR) and nuclear magnetic resonance (NMR) methods. The EPR method is based on the resonant absorption of electromagnetic radiation by paramagnetic particles under magnetic field. The absorption of energy is accompanied by transitions between magnetic sublevels of a system split under the action of the magnetic field. EPR spectra are measured either by varying the frequency of electromagnetic field (usually in the microwave range) at a constant external magnetic field, or by varying the magnitude of an applied magnetic field with the frequency of the alternating electromagnetic field kept constant. Atoms or molecules containing unpaired electrons are in common usage as paramagnetic particles.

The EPR spectrum of an endohedral compound contains information about the chemical state (valence) of an atom or radical encapsulated into the fullerene molecule, about the number of such atoms, as well as about the structure and symmetry of the fullerene shell. So, the number of peaks in an EPR spectrum shows the magnitude of the total spin of unpaired electrons. The resonance absorption frequency is determined by the magnetic field in the region of localization of encapsulated atoms. Thus, the magnetic field can be provided by not only an outer device, but also by the magnetic moment of the nucleus of the given atom or its neighbors. The EPR linewidth determines the relaxation time of the population of the magnetic sublevel of the atom under the action of surrounding particles.

The NMR method has the same physical origin as EPR, but in this case nuclei with nonzero spin I are used as paramagnetic particles. NMR occurs for simultaneous action of two mutually perpendicular magnetic fields — strong constant field H_0 and weak radio frequency field H_1 — on nuclei. The interaction energy between the constant magnetic field and the nuclear magnetic moment is split in accordance with the rule of quantization of moments and, depending on the mutual orientation of these vectors, can take on one of $2I + 1$ integer values. The action of a magnetic field of specific orientation varying with the frequency corresponding to the difference in the energy of some two split sublevels promotes transitions between them accompanied by the resonance absorption of electromagnetic energy.

The magnetic resonance frequency, ranging usually from 10^6 to 10^7 Hz, is proportional to the magnetic field magnitude (H_0) in the region of localization of nuclei under investigation. This field is constituted by the outer magnetic field and fields generated by atomic particles. Thus, the NMR spectrum contains information about all sources of the magnetic field in the local region and specifically about the chemical structure of the compound or crystal structure of the solid material. The number of peaks in the NMR spectrum of a given chemical compound corresponds to the number of chemical states in which atoms of a specific type involved into this compound are found. The width of a peak is determined by the relaxation time of the equilibrium distribution of nuclei over sublevels, which in its turn depends on the spatial distribution of the magnetic field in the region under consideration.

For example, the NMR spectrum of the fullerene molecule C_{60} is determined by the presence in this molecule of some quantity of isotope ^{13}C (natural abundance is about 1%) with a nuclear spin $I = 1/2$ in parallel with atoms of isotope ^{12}C with zero nuclear spin. The chemical state of all

atoms involved in this molecule is absolutely identical: each atom is located at the vertex of one pentagon and two hexagons in a regular manner covering a spherical surface. Therefore, the NMR spectrum of this material contains only one line [4], which provides convincing evidence of such a perfect structure of fullerene. The linewidth of NMR measured in the crystal sample of C_{60} shows the presence or absence of disordered rotation of fullerene molecules in a crystal. Similar measurements performed in a solution provide information about the interaction between fullerene molecules and those of the solvent, which determines the rotation frequency of fullerene molecules. The NMR spectra of higher fullerenes having a lower symmetry contain several peaks related to several different chemical positions of carbon atoms in the molecule. Thus, the NMR spectrum of C_{70} contains five lines. So, NMR spectroscopy provides both quantitative detection of fullerene molecules and discrimination of different isomer modifications of a specific compound.

One more important source of information about the structure and other characteristics of endohedral fullerenes is the optical absorption spectra of these compounds. The comparison of absorption spectra of endohedral and hollow fullerene molecules provides a conclusion about the character of interaction of an encapsulated atom with the surface of a shell, and in some cases about the local position of such an atom. The above-cited work [82] can be taken as a good example of such an analysis, since the optical and ^{13}C NMR spectra of endohedral metal fullerenes were obtained in it, the procedures of synthesis and isolation of which were described above in detail.

3.2 Electronic state of encapsulated atoms

The measured visible and near IR optical absorption spectra of various endohedral metal fullerenes are presented in Fig. 7. As is seen, the spectra related to different metal atoms incorporated into the same fullerene shell have common features. Thus, the optical absorption spectra of $M@C_{80}$ ($M = Ca$, Sr, Ba), depicted in Fig. 7c, show a rise at $\lambda \leqslant 1400$ nm and pronounced common features in the vicinity of 500, 600 and 700 nm. However, these spectra differ considerably from those of the hollow molecule C_{80}, obtained in [83]. They differ also from the spectra of other C_{80}-based endohedral metal fullerenes. In particular, the absorption spectra of $Ce_2@C_{80}$ and $La_2@C_{80}$, in contrast to those given here, show the rise at $\lambda \leqslant 600$ nm and have practically no other features [84]. On the other hand, the measured electron absorption spectra of three isomers of $Ca@C_{82}$ turned out to be practically similar to those of the three isomers of $Tm@C_{82}$, measured in [85]. So, one can conclude that the main distinctive peculiarities in optical spectra of the endohedral molecules are determined by the valence of encapsulated atoms rather than by the structure of the fullerene shell.

The above-formulated conclusion has a common significance. This relates to the behavior of valence electrons belonging to metal atoms encapsulated inside the fullerene cage, which are not localized on the atom orbits, but arranged outside the fullerene surface. The distinction between the optical absorption spectra of endohedral molecules $La@C_{82}$ and $Y@C_{82}$ and those of similar compounds with encapsulated metal atoms of Group II [86] can be explained in the same manner. It is caused by the difference in the valence of metal atoms and respectively in the number of electrons transferred from an atom to a cage. The structure of an endohedral metal fullerene can be expressed in the generalized form as $M_k^{m+}C_n^{m-}$, where k is the number of encapsulated metal atoms, $m = kv$, and v is the valence of the metal atom. It should be kept in mind that the fullerene shell has seemingly no more than six electron vacancies, which limits the total number of transferred electrons m. However, there is experimental evidence of the existence of such charge transfer complexes as $(La^{3+})_2@C_{80}^{6-}$, $(La^{3+})_2@C_{72}^{6-}$ and $(Sc^{2+})_2@C_{84}^{4-}$ [21, 87].

The above-indicated peculiarity in the electron structure of endohedral metal fullerenes already existed at the initial stage of study of these compounds. Thus, the analysis of EPR spectra of endohedral compounds $Y@C_{82}$ and $La@C_{82}$ showed that both yttrium and lanthanum atoms in these compounds are threefold ionized [19]. So, the electronic structure of the compound is expressed through the formula $Y^{3+}@C_{82}^{3-}$ and $La^{3+}@C_{82}^{3-}$. A similar conclusion was made also by the authors of [88] on the basis of X-ray photoelectron spectroscopy data.

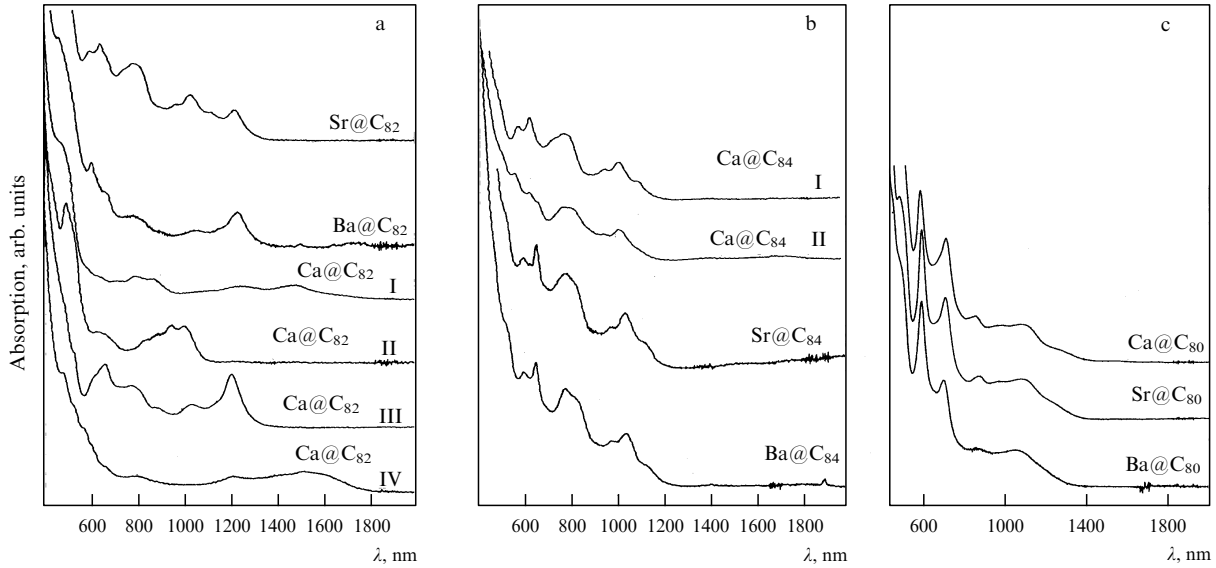

Figure 7. Visible and IR absorption spectra of endohedral metal fullerenes [82].

It should be noted that the above-described concept about the transfer of valence electrons from an encapsulated metal atom onto the outside surface of the fullerene shell has an approximate, qualitative character and, generally speaking, reflects the real situation not quite strictly. This remark can be related to all set of phenomena concerning the origin of the chemical bond, whose quantum nature considerably complicates a simple model of the transfer of a valence electron from a radical-reducer to an oxidizer. Indeed, in accordance with the quantum behavior of chemical systems, the chemical bond can be caused by a partial transfer of the valence electron onto an orbit of a radical-oxidizer, depending on the binding energy of an electron in an atom, its orbital moment and other factors.

This feature is also noted in the case of endohedral fullerenes. Thus, as is shown in [89] using X-ray photoelectron spectroscopy, lanthanum atoms involved in endohedral fullerenes $La@C_{82}$ are inert chemically and characterized by the valence $+3$. However the measurements show that the magnitude of the charge transferred is somewhat less than that for the compound $LaBr_3$. Besides that, it was stated that the electrons transferred from the valence metal shell onto the outside surface of the fullerene cage are subjected to practically full delocalization. A similar conclusion was also made by the authors of [90], who observed the absorption of resonance photons, corresponding to the transition of a 3d electron to the unoccupied 4f orbital of La in the molecule $La@C_{82}$. This phenomenon shows clearly that the valence electrons of lanthanum are transferred to the outside surface of the endohedral molecule not fully, so that there is some probability for electrons to remain in atomic orbitals. Therefore, the electron structure of the system cannot be described in a standard manner as a purely charge transfer complex $La^{3+}@C_{82}^{3-}$. Such a conclusion was also made in [91], where the electron structure of an isomer of the molecule $Tm@C_{82}$ was studied using the photoelectron and X-ray photoemission spectroscopy methods. The measured magnitude of the chemical shift of the Tm 4d state shows that the valence of the thulium atom in this molecule is less than 3. This result was not changed after keeping the sample in open air, which shows the endohedral nature of the compound. The X-ray photoelectron spectra obtained using an undulator synchrotron radiation source show that the electron structure of the endohedral molecule is $Tm^{2+}@C_{82}^{2-}$.

The phenomenon of electron charge transfer from an encapsulated atom onto the outside surface of the fullerene shell is inherent to metal-containing endohedral fullerenes. This phenomenon is not observed if an encapsulated atom is a rare-gas atom or atom with a high ionization potential. Thus, the EPR analysis of the endohedral compound $N@C_{60}$ [46] shows that the electron state of the nitrogen atom in this compound corresponds to the ground configuration $^4S_{3/2}$. This means that the nitrogen atom having the ionization potential 14.5 eV does not suffer any considerable change inside the fullerene cage. A similar situation also persists in the case of an atom of phosphorus encapsulated inside the shell of C_{60} [92], as well as in the cases $F@C_{60}$, $O@C_{60}$ and $N@C_{60}$, according to calculations [93, 94] (the ionization potential of phosphorus is 10.48 eV; that of a fluorine atom is 17 eV, and that of an oxygen atom is 13.6 eV).

The peculiarity of the electron structure of endohedral metal fullerenes relevant to the transfer of the valence electron of a metal atom onto the fullerene shell is reflected basically in the properties of these compounds. Thus, the endohedral fullerenes containing Group II metal atoms have diamagnetic properties, because an encapsulated doubly charged metal ion contains only fully filled electron shells, while the spin moments of valence electrons found on outside orbitals of the fullerene shell are fully compensated. This explains the absence of any relevant signal in the EPR spectrum. The absence of an EPR signal was reported in Ref. [95], where the synthesis and detailed study of the endohedral compound $Eu@C_{74}$ was performed. This shows the charge state of the encapsulated atom to be Eu^{2+}.

The cyclic voltammograms of $Eu@C_{74}$ in a solution of 1,2-dichlorobenzene contain six peaks, four of which correspond to the cathode and two to the anode potential. This result again confirms the conclusion about the divalent state of the Eu atom in the fullerene cage. However, ^{13}C NMR spectra can provide some data about the isomer structure of such molecules, as was done in [79] in relation to the diamagnetic molecule $Sc_2@C_{84}$. The high-resolution ^{13}C NMR spectrum of $Ca@C_{82}$ (isomer III) dissolved in CS_2 was measured over 6 days. It contains 41 lines of equal amplitude situated in the range $135-150$ ppm. In accordance with the analysis performed this shows C_2 symmetry of the isomer. The calculations show seven different structure isomers of C_{82}, three of which have C_2 symmetry. One-dimensional NMR spectroscopy does not provide the discrimination of these three isomers. However, the structure of the most probable isomer is shown in Fig. 8 [82]. The

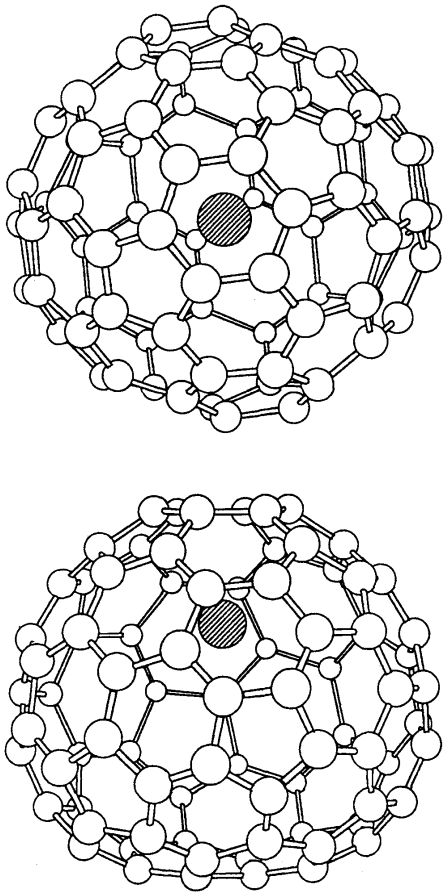

Figure 8. Structure of the $Ca@C_{82}$ molecule (isomer III) determined through fitting the measured ^{13}C NMR spectra to comprehensive quantum mechanical calculation data [82].

computer simulation showed that the Ca atom in this structure is situated on the C_2 axis and off-centered in the direction to the wall of the cage.

It should be noted that the electron state of encapsulated metal atoms is weakly sensitive to the isomer structure of a fullerene shell. This follows, in particular, from the measured photoelectron spectra of isomers $C_{3v}(8)$ and $C_s(6)$ of the molecule $Tm@C_{82}$ [96]. In that work, films of endohedral metal fullerene produced and purified via standard methods were studied. The films were situated on an electron microscope grid inserted into a spectrometer chamber. The films were studied using electron and optical spectroscopy methods. The $K\alpha$ lines of Al (energy 1486.6 eV), Ne (16.8 eV), He (21.2 eV), and He^+ (40.8 eV) with a resolution of 350 meV (for X-ray lines) and 150 meV (for UV lines) were used as a source of radiation. The energy and spectral resolution of EELS measurements were 115 meV and 0.05 Å for the low energy range and 160 meV and 0.1 Å for the case of excitation of the C 1s state, respectively. The Tm 4d absorption edge was measured using the X-ray radiation of electron storage ring. The energy of emitted electrons was measured with a resolution of 70 meV. As follows from the measurements, the photoemission spectra of Tm 4d, measured for two different isomers of C_{82}, are practically indistinguishable. The excitation spectra of 4d electrons measured for two isomers are also identical. The measured value of the binding energy for the 4d electron in the metal fullerene is 172.7 eV, which is about 2.5 eV less than that for trivalent metal thulium. This shows that the valence of thulium in both isomers is less than 3. Further analysis led the authors to the conclusion that the charge state of the atom in both isomers is Tm^{2+}. The analysis of electron spectra showed that the ground electronic state of thulium in both isomers of the metal fullerene corresponds to the configuration $4f^{13}$. Whereas the characteristics of electron states of thulium in endohedral metal fullerenes do not depend on the isomer structure of the molecule, those of carbon (optical energy gap, dielectric constant) are sensitive to this parameter.

A conclusion of the authors of [97] about the weak sensitivity of the electron state of the encapsulated metal atom to the number of atoms enclosed into a fullerene shell is also notable. This conclusion is based on the similarity in X-ray photoelectron spectra of the Pr atom, encapsulated inside the molecules $Pr@C_{82}$ and $Pr_2@C_{80}$. As follows from the comparison of optical absorption spectra of these compounds with those of other endohedral molecules ($La@C_{82}$, $Y@C_{82}$, $Gd@C_{82}$ etc.) [98 – 103], the electron structure of the encapsulated atom is Pr^{3+}. A similar conclusion is related to the compound $Nd@C_{82}$.

3.3 Position of atoms inside the fullerene cage

In the majority of endohedral compounds, the gas-kinetic size of an encapsulated atom is considerably less then the inner size of the fullerene shell. This generates the question about the position of the atom inside the fullerene cage. The answer depends on the magnitude of interaction of the encapsulated atom with the carbon atoms constituting the fullerene structure. The above-considered phenomenon of transferring the valence electrons from an encapsulated atom onto the outer surface of the fullerene shell causes a strong electrostatic interaction between the positive ion formed and the negatively charged shell. This interaction results in an off-center displacement of the equilibrium position of the encapsulated atom (or atoms) inside the shell. Such a displacement was observed for all endohedral metal fullerenes which have been studied.

Thus, the position of yttrium atoms in the endohedral compounds $Y@C_{82}$ and $Y_2@C_{82}$ was found, using the EPR method at room temperature and $T = 10$ K, to be 0.24 and 0.29 nm from the wall, respectively [99]. It is notably less than the average distance between the wall and the geometrical center of the molecule, 0.41 nm. The off-center position of the encapsulated atom in the endohedral molecule $La@C_{82}$ also follows from the treatment of two-dimensional EPR spectra of this molecule dissolved in toluene obtained in the temperature range between 178 K and the room temperature [100].

The off-center displacement of the equilibrium position of an encapsulated atom causes the existence of a quite high permanent dipole moment of endohedral molecules. Thus, the dipole moment of the molecule $Y@C_{82}$ is estimated as 2.5 D [101]. The dipole moment of the molecule $La@C_{82}$ is estimated as 3 – 4 D [89, 102] and for the molecule $Nd@C_{82}$ it is equal to 4 D [103]. The existence of a permanent dipole moment of endohedral metal fullerenes provides relevant materials with specific properties concerning the possible orientation of molecules in a crystal followed by the occurrence of a permanent polarizability. Such crystals should have ferroelectric properties and could be used effectively in electronic devices.

The strong interaction of encapsulated metal atoms with the fullerene shell is also reflected in the structure of endohedral molecules containing more than one incorporated atom. This follows, in particular, from the measured infrared absorption spectra of isomers of $Sc_2@C_{84}$ no. 23 and no. 10 with different symmetries (D_{2d} and D_2, respectively) [104]. The measurements were performed in the spectral range of 80 – 4000 cm^{-1} and temperature range of 80 – 300 K. It has been shown that two scandium atoms in the molecule $Sc_2@C_{84}$ with the symmetry D_{2d} are situated on the twofold symmetry axis 0.403 nm apart from each other and 0.236 nm away from the surface of the fullerene shell. This interatomic distance considerably exceeds that in the crystal lattice; therefore, scandium atoms encapsulated inside the fullerene cage vibrate independently, without dimerization.

A similar conclusion was also drawn by the authors of [105], who measured the ^{45}Sc NMR spectra of $Sc_2@C_{84}$ at frequencies of 121.5 and 72.9 MHz in a temperature range of 238 – 308 K (when CS_2 was used as a solvent) and 293 – 433 K (for *o*-dichlorobenzene as a solvent). The experiments were performed with isomers I and III. The measurements of isomer I at $T \leqslant 363$ K show two different signals of equal intensity, which indicates a difference in the positions of two encapsulated scandium ions. The difference in chemical shifts for these signals is 50 ppm. At $T = 383$ K and higher, the signals merge, which shows the indistinguishabilty of the chemical positions of the two ions. The transition from the state with fixed ion positions to that with indistinguishable positions is caused by the movement of ions inside the fullerene cage. The measured data given in Fig. 9 show a change in of the rate constant of this transition from 1 – 100 s^{-1} at room temperature to 10^4 s^{-1} at 383 K. This provides an estimate for the barrier height characterizing this transition as 0.8 eV (80 kJ/mol). This magnitude is less than the typical binding energy of a normal transition metal atom with a carbon atom (160 – 350 kJ/mol) but considerably exceeds the hydrogen binding energy (4.32 kJ/mol). Due to the Coulomb repulsion, the scandium ions are located far

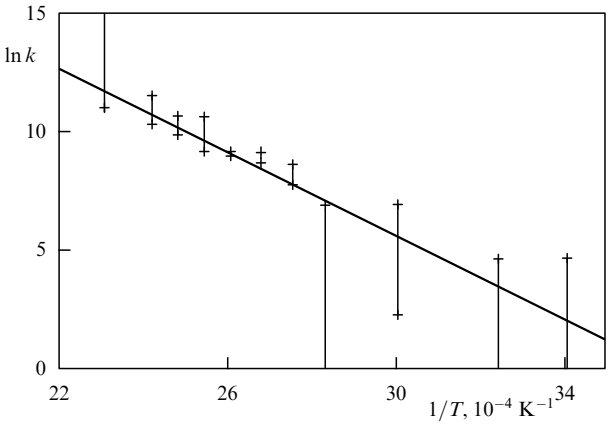

Figure 9. Temperature dependence of the rate constant of the transition of the $Sc_2@C_{84}$ molecule from the state with fixed positions of Sc atoms to that with indistinguishable positions [105].

from each other, being attracted by the negatively charged fullerene shell.

A rise in the temperature activates the movement of encapsulated atoms, which makes their positions indistinguishable at $T > 383$ K. In contrast to isomer I, the NMR spectrum of the isomer III has only one feature in the entire temperature range studied (238 – 433 K). This shows that the states of Sc atoms in this compound are equivalent from the viewpoint of their magnetic environment. This statement is in agreement with the results of the above-cited work [80], where the symmetry of the metal fullerene $Sc_2@C_{84}$(III) was determined as D_{2d} basing on the analysis of NMR spectra, so that Sc atoms occupy equivalent positions in the cage. The relevant molecular structure stated on the basis of measured NMR spectra is shown in Fig. 10.

Scandium atoms in the endohedral molecule Sc_3C_{82} form a regular triangle with equally oriented nuclear spins [15]. This conclusion is evidenced in particular by the character of the EPR spectrum of the compound containing 22 equally spaced lines inherent to the system of three atoms ^{45}Sc having the nuclear spin 7/2.

The transformation in the electron structure of endohedral metal fullerenes related to the transfer of the valence

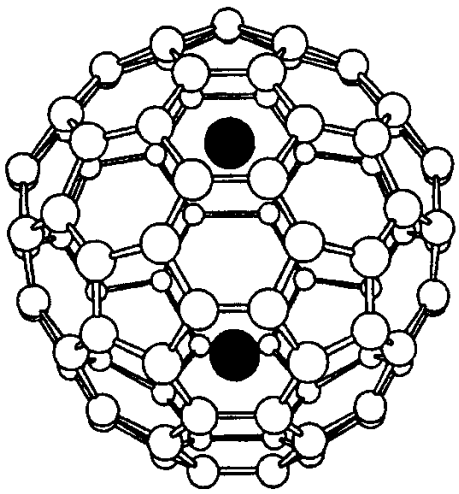

Figure 10. Structure of the $Sc_2@C_{82}$ molecule, determined on the basis of analysis of NMR spectra of these molecules dissolved in CS_2 [80].

electrons of a metal onto the outside surface of the shell region is reflected in such electron parameters of a fullerene molecule as the ionization potential and electron affinity. This can be illustrated by the results of quantum chemical calculation [106] presented in Table 2. As is seen, the incorporation of a metal atom into the fullerene molecule results in a lowering of the ionization potential. On the other hand, the electron affinity of endohedrals is notably higher than that of hollow fullerenes.

Table 2. Ionization potential (E_i) and electron affinity E_a of endohedral and hollow fullerenes calculated for endohedral molecules with different charges on the metal atom [104]

Fullerene	E_i, eV	E_a, eV	Charge on the metal atom in		
			neutral molecule	cation	anion
$Sc@C_{82}$	6.45	3.08	2.16	2.18	2.18
$Y@C_{82}$	6.22	3.20	2.59	2.61	2.60
$La@C_{82}$	6.19	3.22	2.92	2.97	2.90
C_{60}	7.78	2.57			
C_{70}	7.64	2.69			
C_{82}	6.96	3.37			

The fullerene family was extended considerably in the last few years due to the synthesis of *heterofullerene* molecules [107 – 109]. In such molecules one or several carbon atoms that constitute the fullerene cage are substituted, using a chemical procedure, with nitrogen atoms. This results in a considerable lowering in the symmetry of the molecule, which in turn notably changes its physical and chemical properties. Such a change is observed particularly in the behavior of endohedral metal fullerenes, because the properties of a heterofullerene molecule with an encapsulated metal atom are very sensitive to the mutual arrangement of incorporated atoms and nitrogen atoms.

The behavior of metal atoms encapsulated inside the cage of heterofullerenes $La@C_{81}N^+$ and $La_2@C_{79}N^+$ was studied, in particular, in [110]. These molecules were produced as a result of the destruction of the compounds $La@C_{80}(NCH_2Ph)$ and $La@C_{82}(NCH_2Ph)$ by irradiation with high-energy atoms. Further irradiation of endohedral metal heterofullerene molecules causes the successive detachment of two C_2 fragments. In this relation endohedral heterofullerene molecules differ from the hollow heterofullerene molecules $C_{59}N^+$, whose decomposition by high-energy atom irradiation results solely in the detachment of a CN fragment. Such a difference is caused by a considerable redistribution of bonds in the heterofullerene cage as a result of encapsulation of the lanthanum atom. The model calculations performed taking into account the experimental data obtained show that the equilibrium distance between La atoms in the $La_2@C_{79}N$ molecule (0.3585 nm) is less than that for both the molecular ion $La_2@C_{79}N^+$ (0.3622 nm) and the $La_2@C_{80}$ molecule (0.3655 nm). This is caused by the fact, that the 'extra' electron, arising in the $La_2@C_{79}N$ molecule due to the presence of the nitrogen atom, occupies the orbital that determines the La – La bond and shields to some degree the Coulomb repulsion of the charged lanthanum nuclei. In the optimal configuration of $La_2@C_{79}N$, the nitrogen atom is spaced from each lanthanum atom by 0.4518 nm.

On the other hand, the three valence electrons in the molecular ion $La@C_{81}N^+$ are transferred onto the outer

unoccupied electron shells of the fullerene cage as in the case of the molecule La@C_{82}. For this reason the transition from La@C_{82} to La@C_{81}N or from La_2@C_{80} to La_2@C_{79}N, which is accompanied by the appearance of one more electron on the outer fullerene surface, does not result in as prominent a change in the electron structure of the molecule as in the case of pairs of hollow molecules C_{82} and C_{81}N and also C_{80} and C_{79}N, respectively. Therefore, endohedral heterofullerene molecules do not have a noticeable tendency to dimerization that is inherent to the hollow heterofullerene molecules C_{59}N and C_{69}N and is caused by the large degree of localization of electrons in the vicinity of the nitrogen atom position [111 – 114].

If the fullerene shell includes an inert-gas atom, a change in the ionization potential of the molecule is practically unobservable. This is confirmed, in particular, by data relevant to the Ar@C_{60} molecule [35], the ionization potential of which was estimated through the charge exchange reaction

$$\mathrm{Ar@C_{60}^{+}} + \mathrm{A} \rightarrow \mathrm{Ar@C_{60}} + \mathrm{A^{+}}\,,$$

where A is a volatile molecule. The ionization potential of Ar@C_{60} obtained via treatment of measured data using as a volatile molecule 1,4-dimethoxybenzene (ionization potential 7.53 eV) and 1-methylnaphtalene is in the range of 7.53 – 7.8 eV, which corresponds to the ionization potential of C_{60} (7.65 eV). In this property the endohedral rare-gas fullerene molecules differ considerably from metal ones, the ionization potential of which is substantially lower than that for the hollow molecule (thus, in the case of Li@C_{60} this magnitude is 6.3 ± 0.3 eV).

As noted above, if the ionization potential of an encapsulated atom is high, the charge transfer from the atom onto the outer fullerene shell surface does not occur, so that the interaction between the encapsulated atom and the surface is relatively low. This situation persists in the case of the encapsulated atoms such as nitrogen, phosphorus, and fluorine [42 – 49, 92, 93], whose equilibrium state corresponds to the centered position inside the fullerene cage. It follows specifically from the results of the EPR study of the endohedral compound N@C_{60} performed using the standard continuous mode X-band (about 9.4 GHz) spectrometer. The EPR spectra obtained for ^{14}N and ^{15}N are distinguished in extraordinarily narrow lines, which show the spherically symmetric position of the nitrogen atom inside the fullerene cage. The position of the nitrogen atom and the relevant potential energy curve in this compound calculated in Refs [43, 45] are shown in Fig. 11. The vibrational energy quantum evaluated on the basis of this curve is equal to 18.9 meV. This magnitude practically coincides with that (18 ± 1 meV) obtained on the basis of the measured temperature dependence of the EPR line width given in Fig. 12 [45]. The rising shape of the dependence reflects a rise in the number of vibrationally excited endohedral molecules and their increasing contribution to the magnitude of the hyperfine interaction.

Rare-gas atoms encapsulated inside the fullerene shell practically do not interact with it. There have not yet been obtained any direct experimental indications of the position of such atoms inside the shell. However, the equilibrium position of a rare-gas atom inside the fullerene molecule is believed to be the central one, which is caused by the spherical symmetry of the potential energy distribution inside the fullerene shell.

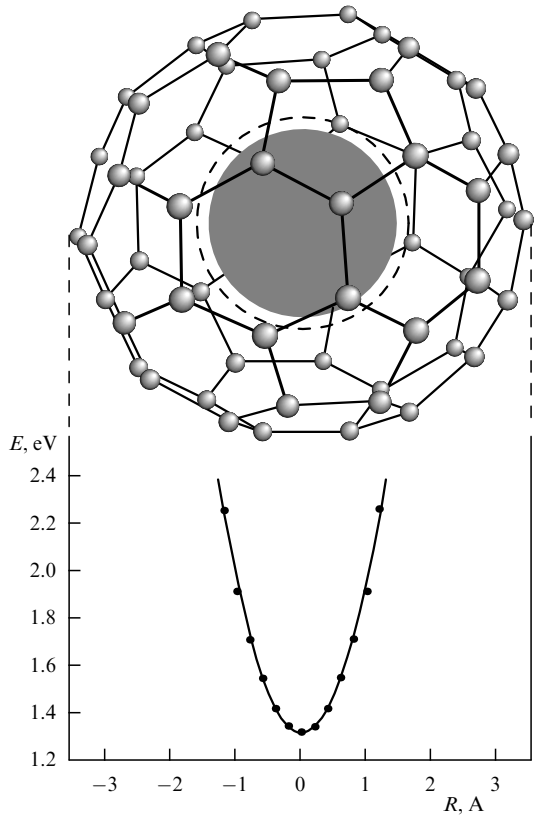

Figure 11. Position of nitrogen atom in the endohedral molecule N@C_{60} as calculated in [43, 45] on the basis of the NMR spectra of this compound.

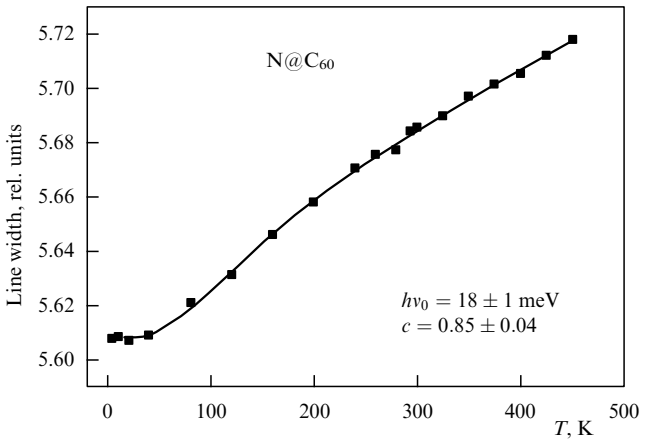

Figure 12. Temperature dependence of the EPR line width of the endohedral compound N@C_{60}, which is the basis for determining the quantum of vibration of the nitrogen atom in relation to the central position [45].

3.4 Dynamics of encapsulated atoms inside a fullerene shell

An atom encapsulated inside a fullerene shell is a quantum mechanical system, which is simulated by a linear harmonic oscillator. Some information about the character of movement of an encapsulated atom inside a fullerene shell can be obtained from the measured NMR spectral linewidth of this atom. An example is the temperature dependences of the ^{45}Sc resonance linewidth for the compound Sc_2@C_{84} measured in [105]. These dependences obtained for isomer III dissolved in CS_2 and *o*-dichlorobenzene having a viscosity differing by

four orders of magnitude are virtually coincident. The independence of the NMR linewidth of the viscosity of solution shows that the line broadening is caused by the inner movement of scandium atoms inside the fullerene shell rather than is related to the rotation of the molecule in solution. Fitting these dependences using the expression $\omega_c = \omega_0 \exp(-E_0/kT)$ (ω_0 is a constant and E_0 is some activation energy) provides the magnitude of this parameter $E_0 = 0.088$ eV for isomer III and about 0.1 eV for isomer I. This magnitude of the activation energy shows the character of binding of the scandium atom with the fullerene shell.

The movement of scandium atoms in the molecule of $Sc_3@C_{82}$ is considerably more free. This follows specifically from the EPR spectra of this compound in a decaline solution measured in the temperature range of 100–330 K [115]. The spectra contain 22 equally spaced lines of equal width corresponding to a projection of the total nuclear spin of $-21/2$, $-19/2$, ..., $19/2$, $21/2$. The distribution of line intensities is in accord with the spin statistics for three Sc nuclei having spin 7/2. The EPR linewidth is about 0.8 G, which is an order of magnitude higher that that measured in earlier work [116]. The analysis of the experimental data shows the origin of the line broadening relevant to the inner motion of metal atoms inside the cage. The barrier height characterizing this motion is estimated as 28 meV and the characteristic reorientation time at 200 K is about 5 ns.

An original method for studying the dynamic behavior and chemical properties of an encapsulated cerium atom in the metal fullerene $Ce@C_{82}$ was realized by the authors of Ref. [63]. This method, called Time-Differential Perturbed Angular Correlation (TDPAC), is based on the measurement of the time correlation of γ quanta of different energy emitted by short-living nuclei of encapsulated atoms. The decay time for the angular correlation corresponds to that of the change in the orientation of an atom inside the fullerene shell. The procedure of synthesis of samples of $^{140}Ce@C_{82}$ is described above. Ce nuclei are formed as a result of the β decay of La. Then the nuclei are excited to the state with an energy 2083 eV, nuclear spin 4, positive parity, and half-life 3.45 ns, which is followed by the relaxation to the ground state accompanied by the emission of γ quanta of energy 389 and 487 keV. The correlation in the angular distribution of these quanta was studied in the temperature range of 10–300 K. The coincidence of two γ quanta emitted at angles 90° and 180° was detected with BaF_2-based scintillation counters. This allowed measurement of the magnitude of the activation energy related to the unfreezing of rotation of endohedral molecules in the solid and dissolved state (1.3 ± 0.1 and 5.9 ± 1.4 kJ/mol, respectively). The difference in the activation energy shows the possibility of formation of solvates, whose decomposition requires energy. At low temperatures, the movement of Ce atoms inside molecules is still observed while the rotation of fullerene molecules is frozen. The authors assign this movement to the recoil effect in the γ emission, which promotes the movement of the Ce atom inside the fullerene cage. The estimated magnitude of the activation energy for this movement (2.3 eV) is in good agreement with calculated data [14].

The above-described method was further developed in the subsequent work of the authors [117], where the intermolecular and intramolecular dynamics of endohedral molecules $CeLa@C_{80}$ in the crystal state were studied via the TDPAC method. Their molecules were formed as a result of the β decay of unstable nuclei ^{140}La, which were generated in a reactor through neutron capture by the ^{139}La nuclei. The β decay results in the formation of a Ce atom. A sample of $La_2@C_{80}$ 1 mg in weight produced and purified using standard methods was soldered into a glass tube and subjected to neutron irradiation in a reactor at a flux of $10^{14}\,cm^{-2}\,s^{-1}$ for 24 h. This promoted the formation of $^{140}La^{139}La@C_{80}$, followed by the β decay and formation of $^{140}Ce^{139}La@C_{80}$. Then the irradiated sample was dissolved in CS_2, purified from contaminants using a filter, and studied using the TDPAC method. The measured temperature dependence of the correlation of the angular distribution of the relevant γ quanta in the temperature range of 10–423 K provides information about the activation energy for the characteristic time of orientation ordering of fullerene molecules in a crystal. These data show the existence of a phase transition related to freezing of the molecular rotation in the crystal at $T = 160$ K. The activation energy for rotation amounted to 3.2 kJ/mol, which is about 2.5 times that for $Ce@C_{82}$ measured in [63]. At $T = 40$ K, the motion of atoms inside the fullerene cage is fully frozen. This conclusion is in contrast with the earlier observation for $Ce@C_{82}$ [63], indicating motion of the Ce atom in the cage even at $T = 10$ K. Probably, the presence of an La atom in the cage of $CeLa@C_{80}$ prevents the motion of the Ce atom.

4. Endohedral fullerites

The intense development of the technology of endohedral fullerene production provides a possibility for studying the physical and chemical properties of crystal structures consisting of these molecules. Such structures are called *fullerites*. At present, the problem of producing pure samples of macroscopic size has been resolved only for higher endohedral metal fullerenes $M_k@C_n$ ($k = 1, 2$; $n = 80, 82, 84$). The number of publications relating to the investigation of properties and behavior of endohedral metal fullerenes in the solid state is relatively small and the information obtained thereby is rather limited. Nevertheless, a clearly pronounced tendency to the widening of the research field of endohedral fullerites permits us to expect the discovery of new interesting properties of this exotic material in the near future.

4.1 Aggregation of endohedral fullerenes

The main distinctions between endohedral metal fullerene molecules and hollow ones concern to two principal peculiarities in their structure that were considered above in detail. The first is caused by the off-center position of the encapsulated atom inside the fullerene cage. This peculiarity provides an endohedral fullerene molecule with a permanent dipole moment, which affects the macroscopic parameters of the relevant fullerite crystal. The interaction potential of molecules having a permanent dipole moment is not spherically symmetric; therefore, a crystal consisting of such molecules should show prominent anisotropic properties. The second peculiarity relates to the charge state of an encapsulated atom and the transfer of valence electrons onto the outside surface of a fullerene molecule. The occurrence of electrons on the outside surface of a fullerene shell determines the character of intermolecular interaction in a crystal. The intermolecular interaction potential contains some contribution of the covalent mechanism along with the van der Waals component.

The permanent dipole moment of endohedral metal fullerene molecules causes a nonspherical character of interaction of such molecules with each other. In turn, this

promotes the formation of elongated structures (aggregates) containing some number of such molecules. Specifically, these structures were observed directly in Ref. [101], where the behavior of $Y@C_{82}$ molecules on a Cu(111) surface with a defect density less than 0.1% was studied. The observations were performed in a vacuum of 6×10^{-11} Torr using a scanning tunneling microscope (STM) equipped with a field ion microscope. The STM observations showed that the molecules retain their mobility on the substrate surface and tend to adsorption on the edges of terraces formed on a surface. The copper substrate is distinct in this respect from Si(111) and Si(100), on which the positions of fullerene molecules are fixed. $Y@C_{82}$ fullerenes form clusters $(Y@C_{82})_n$ $(n = 2-6)$, and in particular, dimers on the substrate surface, even at the initial stage of deposition, when the specific surface density of molecules is rather low. It was stated that the intermolecular distance in the dimer (1.12 nm) is less than the relevant van der Waals distance (1.18 nm). This shows the existence of a strong, non-van der Waals intermolecular interaction in the dimer, caused by the occurrence of the dipole moment ($\sim$2.5 D). Thereby the endohedral molecules show an ability to orientation arrangement, which provides the relevant crystals with anisotropic properties and makes them a promising material from the viewpoint of applications.

The tendency of endohedral fullerenes to surface cluster formation was studied further in [118], where the cluster size distribution functions for the $Y@C_{82}$, $Gd@C_{82}$ and C_{60} fullerenes on a Cu(111) surface were comparatively measured. The purity of the endohedral molecule samples was 99.8%. The formation of fullerene clusters on the substrate surface was observed using a scanning tunneling microscope. Clusters formed along the edge of a terrace on the substrate surface had an elongated structure, which is obviously associated with the nonspherical character of intermolecular interaction. Thus, these clusters are one-dimensional structures. The cluster size distribution function for fullerene molecules of different types is depicted in Fig. 13. As is seen from the graph, this function is nonmonotonic in the case of $Y@C_{82}$, in spite of the rather low coverage of the surface (2.8%), and has a maximum at $n = 2$. This behavior indicates the specific character of the intermolecular interaction of $Y@C_{82}$. The authors of [118] explain the mechanism of this interaction by the presence of three electrons outside the $Y@C_{82}$ fullerene cage with total spin 1/2 (the analog of the lithium atom). This promotes the formation of a dimer, in which an unpaired electrons have opposite spins and undergo the exchange attraction. The binding energies of dimers of $Y@C_{82}$, $Gd@C_{82}$ and C_{60} were estimated on the basis of measured data as 172, 117 and 101 eV, respectively. It should be noted that the given magnitude of the binding energy for the dimer $(C_{60})_2$ is 2.5 times less than the magnitude 0.257 eV [119] obtained through the analysis of temperature dependences of the saturated vapor pressure of this molecule and agreed with many calculated and measured data. This discrepancy is seemingly caused by the action of the conductive substrate.

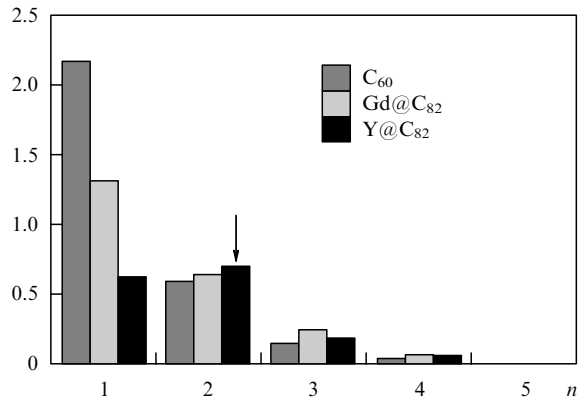

Figure 13. Fullerene cluster size distribution function on a copper substrate surface [118]. The coverage of the surface with fullerene molecules is 4.1%, 3.7% and 2.8% for C_{60}, $Gd@C_{82}$ and $Y@C_{82}$, respectively.

Interesting peculiarities in the aggregation of endohedral fullerenes on the surface of a fullerene film C_{60} were noted in Ref. [103], where the formation of clusters of two-dimensional structure was observed using a scanning tunneling microscope. The purity of samples under investigation was better than 99.9%. The observations showed that the electric field provided by the tip of the microscope probe promoted the arrangement of the film of endohedral molecules $Nd@C_{82}$ in two-dimension ring structures consisting of 6 or 12 molecules on the C_{60} surface. The rearrangement of molecules was observed when the electric field exceeded some critical magnitude ranging between 2.5 and 4 V. This corresponds to an electric field strength between the probe and molecules above 2.5×10^7 V cm^{-1}. The dipole moment of the $Nd@C_{82}$ molecule was evaluated as 4 D, which corresponds to the alignment energy of a molecule in electric field of 180 meV. (A close magnitude of 4.4 ± 0.4 D for the dipole moment of $La@C_{82}$ was found on the basis of the concentration dependences of the static dielectric constant and the refractive index of the solution of $La@C_{82}$ in CS_2 [120].) The six-member ring has an inner diameter of 1.0 ± 0.2 nm, an outer diameter of 3.0 ± 0.2 nm, and a height of 1.2 ± 0.5 nm. This corresponds to a distance between nearest neighbors of 0.9 nm, which is considerably less than that in a close-packed crystal (1.2 nm). The rings can be moved as a whole under the action of the STM tip. These properties of rings permit them to be considered as supermolecules similar to aromatic rings. It is supposed that molecules in the ring are bound with covalent bonds.

The tendency of endohedral fullerenes to aggregation also manifests itself in full in solutions. This behavior is similar to that of hollow fullerenes, whose aggregation in solutions is accompanied with a set of interesting physical phenomena [10]. Thus, in distinction to hollow fullerenes forming clusters only at a sufficiently high concentration of a solution, the phenomenon of aggregation of endohedral fullerenes is observed even in dilute solutions. This is caused by the more effective intermolecular interaction of endohedral fullerenes, having a permanent dipole moment and some number of nonpaired electrons on the surface. The formation of clusters in solutions of endohedral fullerenes results in a notable broadening of NMR lines [54, 116, 121], which is caused by the considerable off-center displacement of the metal atom inside the fullerene cage. Observations show the aggregation of molecules $Li@C_{60}$ and $Li@C_{70}$ dissolved in CS_2 [54], $La@C_{82}$ and $Sc@C_{82}$ dissolved in toluene and CS_2 [116], $La@C_{82}$, $Y@C_{82}$ and $Sc@C_{82}$ dissolved in 1,2,4-trichlorobenzene [111].

The tendency of endohedral fullerene molecules to aggregation is reflected in many properties of these compounds. Thus, the measurements [122] performed in a

temperature range of 1.5–300 K show a significant distinction in the character of the temperature dependence of the specific heat capacity of molecules C_{84}, $Sc_2@C_{84}$, C_{82}, and $La@C_{82}$. These dependences measured for C_{84} and $Sc_2@C_{84}$ have a characteristic two-tiered structure with a bend near $T \approx 50$ K, which indicates a considerable distinction in the energy scale of intermolecular (low energy) and intramolecular (high energy) vibrations. At the same time the temperature dependences of the specific heat capacity of C_{82} and $La@C_{82}$ are close to linear, which is seemingly caused by the effect of molecular aggregation resulting in a higher energy of intermolecular interaction. Another possible reason for the above-described distinction in the behavior of the specific heat capacity of fullerene molecules of different types can be related to the occurrence (in the case of C_{82} and $La@C_{82}$) of a large number of various isomers, the intramolecular vibration spectra of which can differ notably from each other. Thus, the specific heat capacity of such a material is smoothed due to contributions of various isomers.

4.2 Crystal structures of endohedral fullerites

Endohedral molecules are close in size to the relevant hollow molecules; therefore the crystal lattice parameters of endohedral fullerites are close to those of fullerites consisting of hollow fullerene molecules. This conclusion was drawn in the first works [123, 124] related to the study of crystal properties of endohedral fullerite $Sc_2@C_{84}$. The crystals were grown from a solution in CS_2 via slow evaporation of the solvent. Crystals with sizes ranging between 1 and 20 μm were found. High-resolution electron microscopy shows the hexagonal close-packed structure of these crystals with lattice parameters $a = 1.12 \pm 0.02$ nm, and $c = 1.83 \pm 0.02$ nm, $c/a = 1{,}63 \approx (8/3)^{1/2}$. This corresponds to the model of hard spheres with a disordered orientation and unfrozen rotation. The intermolecular distance (1.12 nm) coincides with that found earlier [125, 126] for C_{84} crystal having a face-centered cubic structure. Thus, the encapsulation of two Sc atoms inside the fullerene cage of C_{84} does not result in any noticeable change in the size of the cage estimated as 0.84 nm. The closest distance between the surfaces of $Sc_2@C_{84}$ molecules amounts to 0.28 nm, which is close to that for the C_{60} crystal.

As pointed out above, the encapsulation of a metal atom inside the fullerene cage provides the fullerene molecule with a permanent dipole moment caused by the off-center displacement of the incorporated atom. This is reflected in the crystal structure of the material, which can acquire anisotropic properties. The ordering of endohedral metal fullerene molecules was observed in particular in [127], where the initial stage of crystal growth of endohedral metal fullerene $Nd@C_{82}$ on the surface of a crystal film C_{60} was studied using a scanning tunneling microscope. It has been found that the $Nd@C_{82}$ molecules form a close-packed two-dimensional structure on the surface. Over 60% of molecules form trimers in the form of equilateral triangles of like orientation with respect to the C_{60} film. The authors explain this behavior by the existence of a permanent dipole moment of $Nd@C_{82}$ molecule. The conclusion about the displaced (by about 0.013 nm) position of the molecular dipole moment relative to the symmetry axis was made on the basis of fitting of the experimental data to model calculations taking into account the dipole–dipole interaction of endohedral molecules. Such a displacement is observed only in crystals and is caused by the induced interaction of dipole moments, which moves atoms inside the fullerene cage with respect to the axial position.

The detailed comparison of crystal structures of endohedral metal fullerene $Y@C_{82}$ and the relevant hollow fullerene C_{82} was performed in Ref. [128] using X-ray diffraction analysis. A synchrotron accelerator equipped with a detector in the form of an imaging plate was used as a source of X-ray radiation with a wavelength of 0.1 nm. The exposure time was 1 h. The measurement resolution of 0.29 nm was quite sufficient for determining the position of the encapsulated yttrium atom inside the fullerene cage. The comparison of measured data for polycrystalline powder $Y@C_{82}$ with those for C_{82} powder shows that both crystal structures belong to a monoclinic space group $P2_1$. The lattice parameters are $a = 1.8401(2)$ nm, $b = 1.1281(1)$ nm, $c = 1.1265(1)$ nm, $\beta = 108.07(1)^\circ$ for $Y@C_{82}$, and $a = 1.8241(2)$ nm, $b = 1.1268(1)$ nm, $c = 1.1383(1)$ nm, $\beta = 108.42(1)^\circ$ for C_{82}. The close coincidence between the lattice parameters of metal fullerenes and hollow fullerenes implies the endohedral structure of the former. The somewhat higher (by 1%) magnitude of the parameter c for the endohedral molecule $Y@C_{82}$ in comparison with that of the hollow fullerene C_{82} and, respectively, the somewhat lesser magnitudes of a and b are caused by the dipole–dipole intermolecular interaction in the crystal. In parallel with the crystal structure, the molecular structure of $Y@C_{82}$ was studied using the same method. The analysis of electron density maps obtained showed the shortest distance between yttrium and carbon atoms to be 0.247 nm, which indicated the considerable off-center displacement of the yttrium atom. Besides that, X-ray measurements showed the presence of toluene molecules in both crystal structures ($Y@C_{82}$ and C_{82}), which are situated practically in the middle between two fullerene molecules. The toluene molecules were arranged along the (100) direction in the case of C_{82}, whereas in the case of $Y@C_{82}$ they were arranged along the (201) direction, which showed a strong interaction between endohedral molecules. The analysis of the electron density maps that were determined on the basis of X-ray structure measurements showed the orientation of $Y@C_{82}$ molecules in the crystal as 'head-to-tail' ($Y@C_{82}-Y@C_{82}-Y@C_{82}-Y@C_{82}-Y@C_{82}$...). This is also caused by the presence of the permanent dipole moment of the molecule, promoted by the disturbance of its spherical symmetry (Fig. 14).

As is known [129, 130], the orientation disordering phase transition accompanied by the unfreezing of the rotation of molecules relative to the symmetry axis is inherent to fullerite crystals. This phase transition is caused by some deviation of the molecular form from a perfect sphere and the corresponding distinction of the intermolecular interaction potential from a spherically symmetric one. In the case of the fullerite C_{60}, this transition is observed at $T \approx 260$ K and characterized by a heat of transition $\Delta h = 850$ K. This transition apparently should also take place in the case of endohedral metal fullerites, which are characterized by a higher intermolecular interaction energy. The more considerable deviation of the interaction potential from the spherically symmetric one at a lower temperature should apparently result in a higher thermal effect. However, this conclusion contradicts the measured data [117], showing for the unfreezing of the rotation phase transition in crystalline $^{139}Ce^{140}La@C_{80}$ to occur at a temperature of 160 K with a thermal effect of 380 K. Probably, the reason for this contradiction lies in the fact that rotation of molecules does not disturb their orientation along the axis connecting the encapsulated atoms. In this case one should expect one more phase transition in the crystal of the

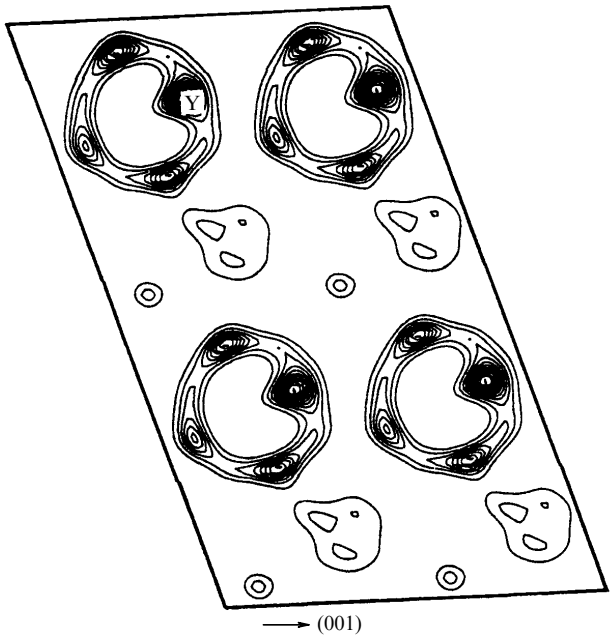

Figure 14. Electron density maps of crystal $Y@C_{82}$ determined on the basis of X-ray structural measurements. The contour lines show the solvent molecules intercalated into the crystal structure [128].

considered type at room or some higher temperature, related to the disturbance of the longitudinal orientation of molecules. Thus, the question about the interrelation between the character of intermolecular interaction and dynamics of molecules in a fullerite crystal requires additional investigation.

Closing the analysis of the physical and chemical properties of crystal structures consisting of endohedral molecules, one should discriminate two kinds of such structures. The first includes endohedral fullerites with encapsulated rare-gas atoms, nitrogen, and some molecules whose structures are in essence very similar to those consisting of hollow fullerenes. First, this relates to the central position of the encapsulated particle inside the fullerene cage, which does not break the spherical symmetry of the fullerene molecule. Second, the electrons belonging to an encapsulated particle are bound strongly with its core and practically do not affect the electron properties of a fullerene molecule. Structures of the second kind, involving mainly endohedral metal fullerites, differ notably from those consisting of hollow fullerenes. This is caused mainly by the off-center displacement of the encapsulated atom in the fullerene cage. This peculiarity of endohedral metal fullerenes results in the occurrence of a permanent dipole moment, providing the crystal with a spatial anisotropy. One more peculiarity of endohedral metal fullerenes, relating to the transition of the valence electron of an encapsulated atom onto the outside shell of fullerene molecule, also considerably affects the character of intermolecular interaction of fullerenes in a crystal. The weak van der Waals interaction is added to by a more intense covalent interaction promoting higher chemical and mechanical stability of the crystal.

5. Chemistry of endohedral fullerenes

The most noticeable change in the chemical properties of a fullerene occurs as a result of encapsulating one or several metal atoms. This is caused by the above-considered effect of transition of valence electrons of the encapsulated metal atom onto the outside surface of the fullerene cage. Such a transition makes a molecule a strong reducer capable of joining adducts that exhibit electron affinity (oxidizers).

The study of photochemical reactions of $La@C_{82}$ dissolved in toluene [131] can be considered an example of the influence of encapsulation of a metal atom on the chemical stability of a fullerene molecule. An extract containing hollow C_{60} and endohedral $La@C_n$ fullerenes dissolved in toluene at concentrations of 1 and 0.76 mg/l was subjected to UV ($\lambda = 254$ nm) and visible ($\lambda = 365$ nm) light irradiation. Mercury-based lamps of low and high pressure were used as a radiation source. The irradiation intensity was 150 mW/cm^2. After irradiation and removal of the solvent, the content of the products was studied using mass spectrometry, EPR spectrometry, and liquid chromatography. The measurements showed that irradiation with visible light for 15 h does not destroy either hollow or endohedral fullerene molecules. The half-life of endohedrals under UV irradiation in the presence of dissolved air was about 1 min, in the absence of air it amounted to about 20 min. The stability of $La@C_{82}$ in relation to UV irradiation is smaller than that for C_{60} by a factor of 100. The stability of endohedral compounds is very sensitive to the presence of dissolved oxygen and also to the presence of optically excited molecules of a solvent.

The thermal stability of endohedral fullerenes is also considerably lower than that of hollow ones. It follows specifically from the results of experiment [132], where the thermal decomposition of the $N@C_{60}$ molecule produced by the ion implantation method was studied. The measurements were performed with both polycrystalline samples and $N@C_{60}$ dissolved in 1-chloronaphtalene, having a high boiling temperature (532 K). The quantity of endohedral molecules in the sample at various temperatures was determined using EPR measurements performed after each 2-K temperature alteration. The measured data shown in Fig. 15 indicate that the stability of $N@C_{60}$ is violated at $T = 480$ K, and these molecules practically do not exist at $T = 590$ K. The results obtained for polycrystalline samples and solutions were similar. According to the model (Fig. 16) [132] based on the dependence of the rate constant of thermal

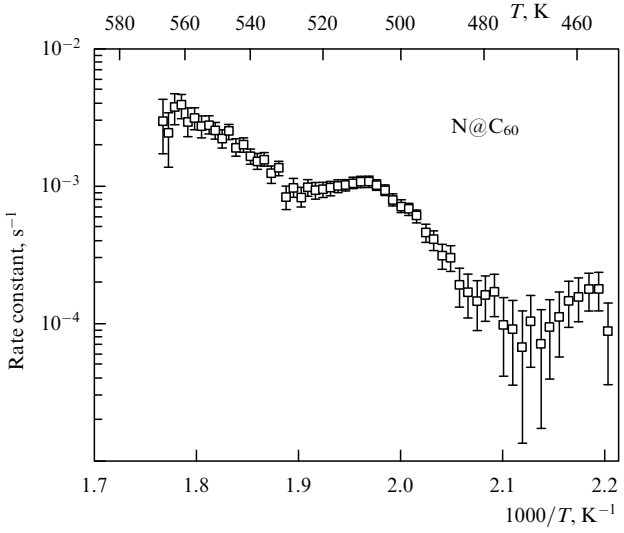

Figure 15. Temperature dependence of the thermal decomposition rate constant of $N@C_{60}$ entering into a crystal sample [132].

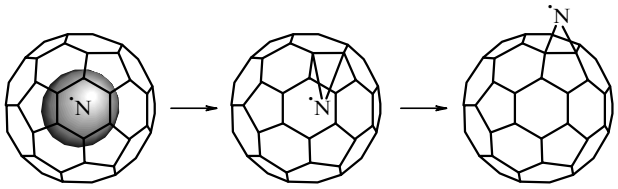

Figure 16. Model of thermal decomposition of the $N@C_{60}$ molecule [132].

decomposition of $N@C_{60}$ on the reciprocal temperature, the decomposition process occurs in two stages. The first is in off-center displacement of the nitrogen atom, resulting in the formation of a bond with two carbon atoms. This is followed by the transition of the atom onto the outside region of the cage. The estimated magnitude of the activation energy characterizing the decomposition is about 1.7 eV.

Table 3 shows the results of comparative experimental studies of the reactivity of endohedral and hollow fullerenes in relation to photochemical and thermal reactions of addition of 1,1,2,2-tetramesityl-1,2-disilane, 1,1,2,2,-tetrakis(2,4,6-trimethylphenyl)-1,2-disilane, digemirane, and diphenyldiazomethane, obtained in [133–138]. The calculated magnitudes of the oxidation and reduction potentials, ionization potential, electron affinity and positions of highest occupied (HOMO) and lowest unoccupied (LUMO) molecular orbitals are also given. Photochemical reactions of addition were performed by irradiating the fullerene solution with light of a tungsten-halogen source in the presence of adduct. The thermal reactions of addition were also performed in a solution. An enhanced reactivity of endohedrals in comparison with hollow fullerenes is caused, on the one hand, by the lower LUMO position and, on the other hand, by the lower magnitude of the reduction potential, which in turn is attributed to the occurrence of valence electrons on the outer surface of endohedral molecules.

The calculation [93] performed for endohedral fullerenes $Li@C_{60}$, $N@C_{60}$ and $F@C_{60}$ using the Hartree–Fock and other quantum mechanical methods shows a direct relationship between the electron structure and the chemical activity of these compounds. While the position of nitrogen and fluorine atoms in these compounds is centered, which is in accord with the neutral state of the atom, the equilibrium position for lithium is off-centered, which corresponds to a value of transferred charge of about 0.6. Therefore, $N@C_{60}$ is similar to C_{60} in its chemical behavior, while in the case of $Li@C_{60}$ the transferred charge is localized mainly on a [6,6]-bond, which results in chemical behavior of this compound similar to that of C_{60} or the isoelectron compound $C_{59}N$. Specifically, this compound forms dimers with a binding energy of 19.4 kcal/mol. Inversely, in the endohedral molecule $F@C_{60}$ the charge transfer occurs from the cage to the fluorine atom. This promotes electron attachment and the formation of endohedral complexes of the kind $F@C_{60}H$ having a binding energy of 20.7 kcal/mol. Adding an adduct results in an off-center displacement of fluorine atom inside the cage.

The influence of adding on the position of an encapsulated atom was studied in detail in [139], where the change in the EPR spectrum of $N@C_{60}$ molecule as a result of addition of diethylmalonate resulting in the formation of the compound $N@C_{61}(COOEt)_2$ was measured. EPR analysis of the product, which was found either in the solution or in a powder form, showed that adding does not destroy the endohedral molecule structure in spite of the rather high chemical reactivity of the nitrogen radical. Dissolved molecules and powder differ noticeably in their EPR spectra. Thus, the spectra of dissolved molecules show a spherically symmetric position of nitrogen atom, while those of a powder sample contain clear indications of an asymmetry caused by the presence of the adduct. Apparently, in the solution some asymmetry is smoothed due to rotation and disordered orientation of molecules. Some information about the position of the encapsulated nitrogen atom is provided by the existence and magnitude of fine splitting of electron states of the nitrogen atom caused by the presence of an adduct. In the absence of an adduct the nitrogen atom is found in the spherically symmetric potential of the fullerene molecule C_{60}. Therefore, its electron wave function is spherically symmetric. Adding violates the symmetry, which removes the degeneration and causes the fine splitting of states with different projections of the moment. Thus, EPR spectra can be used to determine the localization of adducts.

An interesting peculiarity of endohedral fullerenes is the practically total loss of individual properties of an atom encapsulated inside the fullerene shell. This follows specifically from the results of one of the first experiments [140], addressed to determining the chemical properties of endohedral fullerenes. The chemical reactivities of the endohedral molecule $Y@C_{60}$ and molecule YC_{60} in relation to the reaction with molecule NO_2 were compared. $Y@C_{60}$ was produced through the laser sputtering method, while YC_{60} was synthesized in the Fourier-transformation ion cyclotron resonance mass spectrometer. The measurements showed that the yttrium atom involved in the exohedral compound

Table 3. Reactivity in relation to photochemical (*hv*) and thermal (heat) reaction of radical addition, oxidation E_{ox} and reduction E_{red} potentials, HOMO and LUMO positions, ionization potential IP, and electron affinity EA of fullerenes and metal fullerenes [133–138].

	Reactivity		E_{ox}, eV	E_{red}, eV	HOMO, eV	LUMO, eV	IP, eV	EA, eV
	hv	heat						
$La@C_{82}$	+	+	0.07	0.42			6.19	3.22
$Gd@C_{82}$	+	+	0.09	0.39			6.25	3.20
$La_2@C_{80}$	+	+	0.56	0.31	−7.18	−2.55		
$Sc_2@C_{84}$	+	–	0.53	0.97	−6.77	−1.38		
C_{60}	+	–	1.21	1.12	−8.33	−0.63	7.78	2.57
C_{70}	+	–	1.19	1.09	−7.97	−0.84	7.64	2.69
C_{76}	+	–	0.81	0.94	−7.42	−1.13	7.14	3.17
C_{78}	+	–	0.85	0.73	−7.44	−1.49		
C_{82}	+	–	0.72	0.69	−7.36	−1.52	6.96	3.37
C_{84}	+	–	1.04	0.75	−7.79	−1.34		

YC_{60} is oxidized readily, forming YO, while the endohedral complex retains its stability even for an NO_2 concentration excess as high as 1000. This conclusion provides additional evidence of endohedral structure of the molecule. Besides that, a project of utilization of radioactive wastes encapsulating the radioactive atoms inside fullerene cages was developed on the basis of this result. Since fullerenes are not water-soluble, encapsulated atoms can be kept for a long time in underground stores not reacting with the surroundings and not harming the environment. However, the practical realization of such projects is hindered due to the rather high cost of endohedral fullerene production.

6. Filled carbon nanotubes

Shortly after discovery of the fullerenes, the existence was stated of related elongated structures which are cylindrical particles formed of one or several concentric graphite layers [130]. These structures called carbon nanotubes are formed in an electric arc with graphite electrodes in the presence of a buffer gas and under appropriate conditions can account for a considerable part of the cathode surface deposit. The methods for production of carbon nanotubes as well as their structural, electrical, and mechanical characteristics together with a consideration of perspective uses of carbon nanotubes as the basis for development of new technologies are reviewed in detail in [9].

The ideal model of a single-layer carbon nanotube is shown in Fig. 17. The diameter of a typical single-layer nanotube ranges between one and several nm, i.e., somewhat exceeds the diameter of the fullerene molecule C_{60}. The cylindrical surface of a nanotube is inlaid with hexagons, at the vertices of which carbon atoms are situated. The edge part of a nanotube usually has a hemispherical structure. The structure of hemispheres closing a nanotube involves not only hexagons but also six pentagons, so that each hemisphere can be considered as a half of a fullerene molecule. Thus, a carbon nanotube closed from two sides can be considered as an elongated fullerene molecule.

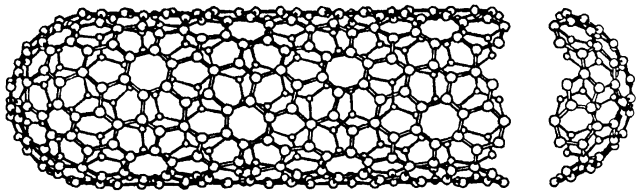

Figure 17. Ideal structure of a carbon nanotube.

Shortly after the discovery of the carbon nanotubes the attention of researchers was attracted to a problem related to the possibility of filling nanotubes with various substances. This problem has not only a purely scientific interest but also an important applied significance, because a nanotube filled with a conductive, semiconductive, or superconductive material may be considered as the tiniest element of microelectronics familiar to us today. The basic scientific interest in this problem is caused by the possibility of obtaining an experimentally justified answer to the question: at what minimum tube size do the capillary phenomena hold their peculiarities inherent to macroscopic objects? If a nanotube can be considered as a strongly elongated fullerene molecule, then a nanotube filled with a substance is nothing but a strongly extended endohedral structure. That is why the problem of producing and studying carbon nanotubes filled with a substance relates closely to that of endohedral fullerenes.

6.1 Capillary effects

It is conceivable that this subject was first considered in Ref. [142], where the problem of the molecule HF being drawn inside a nanotube under the action of the polarization forces was analyzed theoretically. It was supposed that the capillary phenomena resulting in drawing-in liquids wetting the inner surface of a capillary retained their nature on transferring to tubes of nanometer diameter.

The filling of nanotubes with various substances has been made possible as a result of the development of a method for opening one of the ends of a nanotube through the action of a strong oxidizer [143]. In this case a fusible molten metal (lead) penetrates inside an open-ended nanotube due to the effect of capillary action. In this experiment [143] an electric arc at a voltage of 30 V and 180 – 200 A current designed for nanotube production was ignited between the electrodes 0.8 cm in diameter and 15 cm in length. As a result of thermal decomposition of the anode surface, a material forming a layer 3 – 4 cm in height was deposited on the cathode surface. This substance was extracted from the chamber and conditioned at $T = 850\,^{\circ}\mathrm{C}$ for 5 h under flowing carbon dioxide. This procedure resulted in a weight loss of about 10% and promoted the removal of amorphous graphite particles from the sample surface and the opening of nanotubes contained in the deposit. The interior of the deposit containing nanotubes was introduced into ethanol and ultrasonicated. The product of oxidation dispersed in chloroform was then deposited onto a carbon tape with holes made to permit transmission electron microscope observations. The latter showed that untreated tubes possessed a seamless structure, regular cap shape, and a diameter ranging between 0.8 and 10 nm. The oxidation resulted in damage of the caps for about 10% of nanotubes and in partial stripping of the layers around caps. The sample containing nanotubes to be examined was filled in a vacuum with molten lead droplets produced by irradiating a metal surface with an electron beam. Lead droplets ranging from 1 to 15 nm in size were observed on the outer surfaces of nanotubes. The latter were annealed for 30 min in air at $T = 400\,^{\circ}\mathrm{C}$ (higher than the melting point of lead). As shown by the electron microscope observations, a portion of nanotubes were found after annealing to be filled with a solid material. A similar effect of tube filling was observed on irradiating the tube caps opened as a result of annealing with a powerful electron beam. A sufficiently strong irradiation resulted in the melting of material located near the open end of a tube and its penetration into the tube. The occurrence of lead inside tubes is indicated by the X-ray diffraction and electron spectroscopy methods. The thinnest lead wire is 1.5 nm in diameter. The observations showed that the portion of filled nanotubes did not exceed 1%.

The subsequent efforts of researchers in the direction considered were addressed to a detailed study of the peculiarities of capillary phenomena in carbon nanotubes, which manifest themselves in filling nanotubes with substances of varied nature. The results of these studies show an interconnection between the magnitude of the surface tension of a substance and its ability to be capillary drawn inside a carbon nanotube. Some of these data are generalized in

Table 4 [144], where the stated experimental ability of various liquid substances to be capillary drawn inside carbon nanotubes is correlated with the magnitude of their surface tension. As is seen, the capillary properties of nanotubes show themselves only in relation to materials, having a rather low (less than 200 mN/m) magnitude of surface tension in the liquid state. This conclusion is in agreement with a qualitative analysis of the phenomenon performed by Ebbesen [144, 145].

Table 4. Wetting properties of nanotubes (the temperature is close to the melting point; the lead and bismuth oxide stoichiometry is uncertain) [144].

Substance	Surface tension, $mN\,m^{-1}$	Capillary effect
HNO_3	43	Yes
S	61	Yes
Cs	67	Yes
Rb	77	Yes
V_2O_3	80	Yes
Se	97	Yes
Lead oxides	($PbO \sim 132$)	Yes
Bismuth oxides	($Bi_2O_3 \sim 200$)	Yes
Te	190	No
Pb	470	No
Hg	490	No
Ga	710	No

Analyzing experiments related to the investigation of the capillary phenomena in nanotubes, attention should be paid to the role of oxygen, whose presence often determines experimental results. Thus, the experiments directed to nanotube filling with lead and bismuth in a vacuum have failed, whereas similar experiments performed in the presence of atmospheric air have resulted in the occurrence of the capillary effect. This observation is quite explicable from the viewpoint of the above-expounded consideration of the correlation between the capillary phenomena and the magnitude of the surface tension of the melt. The surface tension of molten lead and bismuth oxides is much less than that for pure molten metals; therefore, the presence of oxygen producing oxides promotes the occurrence of capillary phenomena.

As noted in Ref. [146], for the manifestation of the capillary effect in relation to liquid metals with a high surface tension it is insufficient to use the standard procedure described above. In such a case it should be added with special contrivances. One method aimed at solving this problem is in applying an outer pressure which permits the pushing out force to be overcome. Another way, proposed and realized in Refs [147, 148], is based on the use of solvents having a low surface tension and for this reason capable of penetrating inside nanotubes due to the capillary effect. The authors used concentrated nitric acid quite effectively as a solvent which is characterized by a rather low magnitude of surface tension (about $43\ mN\,m^{-1}$). Soot containing nanotubes was produced by electric-arc graphite vaporization. The productivity of the facility was about 15 g/h of a cathode deposit containing up to 25% nanotubes along with carbon nanoparticles. 2 g of deposit was inserted into 45 g of 68% nitric acid and was conditioned at a temperature of $T = 240\,^{\circ}C$ for 4.5 h. After drying, the insoluble substance was ultrasonicated in chloroform and dried again in a vacuum. The tunneling electron microscopic images of the resulting material show about 80% of the nanotubes to be opened. Treatment with nitric acid for 24 h resulted in the opening of about 90% nanotubes. For filling nanotubes with a metal dissolved in nitric acid, a suspension containing 0.4 g of closed nanotubes and 20 g of nitric acid solution involving 1 g of hydrated nickel nitrate was prepared. The suspension was conditioned at a temperature of $T = 140\,^{\circ}C$ for 4.5 h. After filtration and drying, the sample was heated to $T = 450\,^{\circ}C$ with flowing He and annealed at the same temperature for 5 h. As follows from the observations, this promoted the opening of 80% of nanotubes, 60–70% of which contained a nickel material. A similar material was also formed on the outside surfaces of nanotubes and nanoparticles. The crystal structure of this material corresponds to NiO. Crystals of NiO located inside the nanotubes are 3–6 nm in diameter and up to 30 nm in length. They are usually situated rather far from the open ends of the nanotubes. The treatment of closed nanotubes with uranyl nitrate dissolved in nitric acid permitted the investigators to produce nanotubes filled with an uranium-bearing substance that contained 70% uranium oxide. Similar results were obtained for Fe and Co. The treatment of samples containing Ni, Co and Fe oxides with hydrogen at a temperature of $400\,^{\circ}C$ for 4 h seemingly caused the reduction of metal crystals from oxides. The processing of nanotubes filled with uranium oxides with an aqueous solution of nitric acid resulted in the dissolution of most of the uranium-containing crystals and their escaping from the nanotubes. In filling the nanotubes, solutions of metals and their oxides in nitric acid were used. So, nitric acid plays a twofold role: opening nanotubes and encouraging the metal penetration inside. The low magnitude of the surface tension of nitric acid is used in the process, which in accordance with the considerations given above should wet the inner nanotube surface.

6.2 Synthesis of filled nanotubes

The most natural method for production of nanotubes filled with metals and compounds of them is based on the technology of catalytic nanotube synthesis using metals as catalysts. In so doing, the nanotubes are filled with metals and compounds in the process of synthesis, which permits the above-indicated limitations related to the magnitude of the surface tension of molten metals to be avoided. Such an approach usually results in multilayer nanotubes fully or partly filled with crystals of metals, their oxides or carbides. The list of elements that were introduced inside nanotubes in such a manner involves metals such as Rh, Pd, Pt, Mn, Co, Fe, Ni, Sc, La, V, Ce, Zr, Y, Ti, etc. as well as compounds of them. A considerable variety of crystal forms and chemical states for encapsulated metals should be noted. Thus, in Ref. [149], where the iron-group metals (Fe, Co, Ni) were used as a catalyst in the synthesis, not only crystalline metal particles (bcc Fe, fcc Co, fcc Ni), but also carbides X_3C (X is the metal atom) were found inside nanotubes.

Special attention should be paid to Ref. [150], where carbon nanotubes filled with a superconductive material TaC were produced. The success of this experiment has opened a perspective for using carbon nanotubes in superconductivity technology. To produce encapsulated TaC crystals, powdered Ta of purity 99.9% and finely ground graphite were mixed in a weight ratio of ~ 0.6 and pressed into a hollow graphite rod (8 mm in length, 3 mm in inner diameter and 6 mm in outer diameter) used as an anode. An arc was burnt in an He atmosphere at a pressure of 100–300 Torr, a

voltage of 30 V, a current of 30 A, and the interelectrode gap of 2 – 3 mm. The fixed cathode was 17 mm in diameter. The temperature of the end cathode surface was estimated as 1500 °C. Under the action of the discharge, a carbon deposit with admixture of TaC particles was formed on the cathode surface; the particles were found both on the surface and in the bulk of the deposit. To extract the TaC particles incorporated into graphite shells, the deposit samples (100 mg) were placed into 75% solution of sulfuric acid and held at a temperature of 80 °C for two weeks. As a result of this procedure, the nonencapsulated particles were fully dissolved in the acid. The rest of the particles were repeatedly washed with distilled water, dried and dispersed using ultrasonication in ethanol. Afterwards, one – two drops of a suspension were placed with a dropper onto a carbon-coated copper grid for making electron-microscopic observations. As follows from the observations, the cathode deposit contains a large quantity of TaC crystals encapsulated in nanotubes, and a handful of crystals encapsulated in elongated or compact polyhedrals. In the substance taken from the partly sputtered anode surface, by contrast, a large quantity of particles enclosed in polyhedral cells and a small quantity of short nanotubes were found. In what follows, attention will be paid to particles extracted from the cathode deposit. TaC particles ranging from 2 to 20 nm in size with a maximum in the distribution function at 6 nm are usually enclosed in multi-shell nanotubes with an interlayer spacing of 0.3481 nm, which is 3.9% higher than for pure graphite. The structure of the encapsulated TaC was studied using the X-ray diffraction method. This structure is not different from the conventional crystal structure of TaC (NaCl structure type) with a lattice parameter $a_0 = 0.4455$ nm. The superconducting transition was observed at $T = 10$ K through magnetic susceptibility measurements. The distinctive feature of TaC is its extraordinarily high melting point (3985 °C), which is the maximum among all carbides and much over the melting point of pyrolythic graphite (2500 – 3500 °C). This permits us to believe that a carbon nanotube enclosing a tantalum carbide particle is formed after the carbide crystallization.

One more interesting method for the production of nanotubes filled with a metal was demonstrated in Ref. [151], where the gaseous iron compound $Fe(CO)_5$ was used as a metal-containing agent. A graphite-electrode arc was burnt in a mixture of He (50 mbar) and $Fe(CO)_5$ (50 – 200 mbar), which dissociated at high temperature, releasing Fe. The interelectrode voltage was 20 V and the current was 100 A. The soot produced in the gaseous phase as a result of the discharge was dispersed in alcohol and then mounted on a copper grid for making electron-microscopic observations. In the soot collected from the chamber walls, fullerenes were observed along with carbon particles containing particles of iron and iron carbides. The iron content was varied through the change in the temperature of the reservoir with liquid $Fe(CO)_5$, which determined the partial pressure of this gas. The chemical analysis of soot taken from the chamber walls showed an iron concentration ranging from 1.8 to 12 wt. %. The soot contained iron nanoparticles incorporated into a graphite envelope and also a large amount of multilayer carbon nanotubes partly filled with iron. The diameter of the nanotubes ranged between 20 and 65 nm, and their length reached 2.5 μm. The shape of the tubes was far from linear; they were filled with a metal only partly, but not over all their length. Nevertheless, the interlayer spacing was always equal to 0.34 nm. The metal enclosed in the nanotubes had either a single crystal or polycrystalline structure. In some cases, inclusions of FeC and Fe_3C (cementite) were observed

The most detailed study of the peculiarities of filling carbon nanotubes with various metals is presented in Ref. [152], whose authors performed experiments resulting in the encapsulation of 17 various metals inside nanotubes. The experimental setup was described in detail in a preceding work by the same authors [153]. Graphite rods 9 mm in diameter and 42 and 72 mm in length were used as an anode and a cathode, respectively. The hole 6 mm in diameter and 38 mm in depth drilled in the anode was filled with a mixture of graphite and metal powders. The arc burnt for 30 – 60 min at an interelectrode separation of several mm, current of 100 – 110 A, voltage of 20 – 30 V and He pressure of 450 Torr. The experimental data are given in Table 5. Two modes of nanotube filling with metals may be distinguished. The first is observed in the case of Cr, Ni, Dy, Yb and Gd. In this case, the nanotubes are uniformly filled lengthwise with a metal, forming a wire of constant diameter that is aligned strictly in parallel with the axis of the tube. These are true metal wires ranging from 100 nm to over 1 μm in length, surrounded with a graphite envelope. The second kind of filling is observed in the case of Pd, Fe, Co, and Ni. In this case, the nanotubes are filled incompletely along their full length with a metal, which may be found as encapsulated particles located from place to place along the nanotube length and near its cap. The nanotubes nonuniformly filled with a metal over the length have a variable diameter, although the graphite layers remain aligned along the tube axis. In all cases but Co and Cu, where the nanotubes are filled with a pure metal forming a face-

Table 5. Experimental data related to filling nanotubes with metals [151, 152].

Element	Ti	Cr	Fe	Co	Ni	Cu	Zn	Mo	Pb	Sn	Ta	W	Gd	Dy	Yb	Sm
Size of the metal grain, μm	10	5	1	2	10	40	10	10	1	20	40	5	400	400	400	
Boiling point, K	3562	2945	3135	3201	3187	2836	1180	4912	3237	2876	5731	5828	3539	2835	1467	
Filling of nanotubes	–	+	+	+	–	–	–		–	+	+	+	+	–	–	+
Unfilled shells	–	+	+	+	+	–	–	–	–	+	+	+	+	–	–	+
Length of the filled section of a tube, nm		3000	200	200	1000				1000	3000	200	200	1200	600	200	10
Number of holes	0	7	5	3	2	0	0		2	0	0	0	7	5	1	9

centered cubic crystal structure, the metal is present in the form of a carbide. Thus, the carbides Fe_3C (cementite), Ni_3C, and TiC have been identified.

As is seen from the experimental data presented in Table 5, the formation of metal nanowires inside carbon nanotubes does not depend on the boiling point of the metal. This means that in the first stage of nanotube synthesis the temperature of the arc in the region of vaporization exceeds the boiling point of the metal and graphite. The observed correlation between the formation of nanowires and existence of unfilled electron shells in metal atoms shows that the metal ions in the process of nanotube filling are found in the most stable oxidizing state. As is seen from Table 5, the more vacancies in the unfilled electron shells, the greater the length and higher the quality of nanowires. Thus, Cr and Gd are the best metals for nanowire production, having the maximum number of vacancies in the unfilled electron shells and forming the longest wires.

Carbon nanotubes can be filled not only with liquid but also gaseous substances. Such a possibility was shown in Ref. [154], where the results of experiments relating to single-layer nanotube filled with molecular hydrogen were presented. These results are of great practical significance, because they open a possibility for solving the practically important problem of the safe storage of hydrogen used as a fuel in ecologically pure car engines. A soot containing single-layer nanotubes was synthesized in an electric arc with graphite electrodes doped with powdered cobalt. In this case, fibers several μm in length, consisting of 7–14 single-layer nanotubes (near 1.2 nm in diameter) bound into bundles, were obtained. Besides that, Co nanoparticles were also present, ranging from 5 to 50 nm in size, incorporated into amorphous carbon. The content of Co was about 20 wt. %. The samples of soot containing single-layer nanotubes together with those of activated charcoal used for comparison were placed into platinum-foil packages equipped with holes to ensure gaseous diffusion. These samples were kept in hydrogen at a pressure of 300 Torr and a temperature of 273 K for 10 min, and in some cases more than 3 min at the same pressure and a temperature of 133 K, afterwards they were cooled down to 90 K and evacuated. The H_2 content in the samples was determined using the method of programmable thermal desorption. As follows from measurements, the intensity of the hydrogen desorption from the soot containing nanotubes is about 10 times higher (at the same temperature) than that for activated charcoal. The activation energy for desorption is estimated as 19.6 kJ/mol.

A remarkable example of the phenomenon of filling the nanotubes with a substance relates to filling single layer nanotubes with fullerene molecules performed recently [155, 156]. A sample of a soot produced as a result of laser sputtering of a graphite surface and containing fullerene molecules C_{60} along with single-layer nanotubes was subjected to heat treatment at $T = 1100\,^{\circ}C$ for 14 h; 1–2 mg of this sample was added to 4 ml of a mixture of 90% sulfuric acid and 70% nitric acid (3:1), after which the suspension produced was held at $T = 90\,^{\circ}C$ for 10 min. After repeated washing and drying, the solid substance was examined using high-resolution transmission electron microscope. To obtain the absorption optical spectra, the material was placed into toluene. The measurements showed that the material under investigation contained single-layer nanotubes about 1.4 nm in diameter partially filled with chains of C_{60} molecules. The distance between the centers of molecules is about 1 nm, which corresponds to the relevant value in the fullerite crystal. The degree of filling of nanotubes with fullerene molecules approaches 5.4%.

7. Conclusions

Closing the consideration of problems that concern the production and investigation of endohedral fullerenes and related structures, one can conclude that the evolution of the indicated set of problems for a short time period has resulted in the formation of a new quickly developing direction of chemical physics. The interest in this direction from many research groups is mainly fundamental and is caused by the possibility of artificially controlling the molecular structure as well as studying the consequences of such control. Thus, in parallel with the known methods of incorporation of atomic particles inside the fullerene cage based on the use of high pressures, ion beams, or nuclear reaction products, one more interesting possibility is considered [16]. This is based on the use of chemical methods of creating a 'window' in a fullerene cage followed by filling the cage with atomic particles and closing the shell. Practical realization of this program can provide a qualitative alternative to the traditional outlook on the origin of chemical synthesis and considerably widen the family of endohedral structures synthesized artificially.

The state of atomic particles enclosed inside a fullerene shell is unique and cannot be reproduced in any another way. Thus, metal atoms partly or fully transfer their valence electrons to the outside part of the fullerene cage, practically losing their chemical individuality. This determines the off-center position of an atom inside a fullerene cage, providing the endohedral molecule with a permanent dipole moment. The electron shells of encapsulated rare gas, nitrogen, fluorine atoms etc., remain practically unchanged, which determines the central position of these atoms inside the cage. The investigation of properties of such particles considerably widens our outlook concerning the behavior of quantum subjects in extraordinary conditions. The investigation of capillary phenomena observed in filling carbon nanotubes with liquid metal is of fundamental interest. The diameter of a nanotube is only several times as large as the atomic size, and the fact that capillary phenomena even on this small scale retain their major qualitative features should be considered as a notable contribution to the physics of fluids.

The possibilities of direct practical applications of endohedral structures in technologies and physical instrumentation are at present rather limited, which is caused first of all by the very high cost of manufacturing these structures. In this relation, the most promising for applications are, seemingly, filled nanotubes for use for gas storage, as nanowires, and others elements of nanoelectronic technologies, which are attracting the attention of many research groups. Although these possibilities are still far from practical realization, even now one can note the stimulating influence of the development of the direction considered upon such fields of chemical physics as liquid chromatography, NMR and EPR spectroscopy, high-resolution tunneling electron microscopy, etc.

Thus, endohedral structures represent a new class of nanometer-size objects, showing extraordinary physical and chemical properties and having a great potential for practical use. Undoubtedly, in the near future one can expect discovery of new interesting peculiarities in the behavior of these objects

as well as the realization of potential possibilities of their practical application.

The author thanks B M Smirnov for fruitful criticism. The work was supported in part by INTAS (grant 97-11894).

References

1. Kroto H W et al. *Nature* (London) **318** 162 (1985)
2. Smolli R E *Usp. Fiz. Nauk* **168** 323 (1998)
3. Kerl R F *Usp. Fiz. Nauk* **168** 331 (1998)
4. Kroto G *Usp. Fiz. Nauk* **168** 343 (1998)
5. Krätschmer W et al. *Nature* (London) **347** 354 (1990)
6. Eletskiĭ A V, Smirnov B M *Usp. Fiz. Nauk*. **161** (7) 173 (1991) [*Sov. Phys. Usp*. **34** 616 (1991)]
7. Eletskiĭ A V, Smirnov B M *Usp. Fiz. Nauk*. **163** (2) 33 (1993) [*Phys. Usp*. **36** 202 (1993)]
8. Eletskiĭ A V, Smirnov B M *Usp. Fiz. Nauk*. **165** 977 (1995) [*Phys. Usp*. **38** 935 (1995)]
9. Eletskiĭ A V *Usp. Fiz. Nauk*. **167** 945 (1997) [*Phys. Usp*. **40** 899 (1997)]
10. Bezmel'nitsyn V N, Eletskiĭ A V, Okun' M V *Usp. Fiz. Nauk*. **168** 1195 (1998) [*Phys. Usp*. **41** 1091 (1998)]
11. Heath J R et al. *J. Am. Chem. Soc*. **107** 7779 (1985)
12. Taylor R et al. *J. Chem. Soc. Chem. Commun*. 1423 (1990)
13. Chai Y et al. *J. Phys. Chem*. **95** 7564 (1991)
14. Nagase S et al. *Chem. Phys. Lett*. **201** 475 (1993)
15. Bethune D S et al. *Z. Phys. D* **26** 153 (1993); *Nature* (London) **366** 123 (1993)
16. Hirsch A *The Chemistry of the Fullerenes* (Stuttgart: G. Thieme Verlag, 1994)
17. Guo T et al. *Science* **257** 1661 (1992)
18. Johnson R D et al. *Nature* (London) **355** 239 (1992)
19. Hoinkis M et al. *Chem. Phys. Lett*. **198** 461 (1992)
20. Yannoni C S et al. *Science* **256** 1191 (1992); *Synth. Metals* **59** 279 (1993)
21. Stevenson S et al. *J. Phys. Chem. A* **102** 2833 (1998)
22. Bandow S et al. *J. Phys.Chem*. **97** 6101 (1993)
23. Fuchs D, Adelman P, Michel R, in *Progress in Fullerene Research. Int. Winterschool on Electronic Properties of Novel Materials, Austria, 1994* (Eds H Kuzmany et al.) (Singapore: World Scientific, 1994) p. 108
24. Shinohara H et al. *J. Phys. Chem*. **98** 8597 (1994)
25. Bandow S et al. *J. Phys. Chem*. **96** 9609 (1992)
26. Lebedkin S et al. *Appl. Phys. A* **66** 273 (1998)
27. Pradeep T et al. *Ind. J. Chem. A* **31** F17 (1992)
28. Mieno T *Jpn. J. Appl. Phys*. **37** (2) L762 (1998)
29. Mieno T, Dewa T, Sakurai A, in *Proc. XXII ICPIG, Hoboken, USA 1995* Vol. 1, p. 89
30. Mieno T *Jpn. J. Appl. Phys*. **35** L591 (1996)
31. Saunders M et al. *Science* **259** 1428 (1993); **271** 1693 (1996)
32. Khong A et al. *J. Am. Chem. Soc*. **120** 6380 (1998)
33. Saunders M et al. *Chem. Phys. Lett*. **248** 127 (1996)
34. Saunders M et al. *J. Am. Chem. Soc*. **116** 2193 (1994)
35. DiCamillo B A et al. *J. Phys. Chem*. **100** 9197 (1966)
36. Saunders M et al. *Nature* (London) **367** 256 (1994)
37. Saunders M et al. *J. Am. Chem. Soc*. **117** 256 (1995)
38. Saunders M et al. *J. Am. Chem. Soc*. **116** 3621 (1994)
39. Brink C et al. *Chem. Phys. Lett*. **286** 28 (1998); **290** 551 (1998)
40. Christian J J, Wan Z, Anderson S L *Chem. Phys. Lett*. **199** 373 (1992)
41. Christian J J, Wan Z, Anderson S L *J. Phys. Chem*. **96** 10597 (1992)
42. Murphy T A et al. *Phys. Rev. Lett*. **77** 1075 (1996)
43. Weidinger A et al. *Appl. Phys. A* **66** 287 (1998)
44. Knapp C et al. *Chem. Phys. Lett*. **272** 433 (1997)
45. Grupp A et al., in *Molecular Nanostructures* (Eds H Kuzmany et al.) (Singapore: World Scientific, 1998) p. 224
46. Pietzak B et al. *Chem. Phys. Lett*. **279** 259 (1997)
47. Weidinger A et al., in *Molecular Nanostructures* (Eds H Kuzmany et al.) (Singapore: World Scientific, 1998) p. 173
48. Murphy T A et al., in *Fullerene and Fullerene Nanostructures* (Eds H Kuzmany et al.) (Singapore: World Scientific, 1996) p. 190
49. Pietzak B et al., in *Molecular Nanostructures* (Eds H Kuzmany et al.) (Singapore: World Scientific, 1998) p. 180
50. Tellgmann R et al. *Nature* (London) **382** 407 (1996); in *Fullerenes and Fullerene Nanostructures* (Eds H Kuzmany et al.) (Singapore: World Scientific, 1996) p. 168
51. Krawez N et al., in *Molecular Nanostructures* (Eds H Kuzmany et al.) (Singapore: World Scientific, 1998) p. 180
52. Kusch Ch et al. *Appl. Phys. A* **66** 293 (1998)
53. Campbell E E B et al. *J. Phys. Chem. Solids* **58** 1763 (1997)
54. Gromov A et al. *Chem. Commun*. 2003 (1997)
55. Campbell E B B et al. *Chem. Phys*. **239** 299 (1998)
56. Yoshi K et al. *Appl. Phys. Lett*. **61** 2782 (1992)
57. Ohtsuki T et al. *Phys. Rev. Lett*. **77** 3522 (1996)
58. Ohtsuki T et al. *Phys. Rev. Lett*. **81** 967 (1998)
59. Gadd G E et al. *Chem. Phys. Lett*. **270** 108 (1997)
60. Gadd G E et al. *Chem. Phys. Lett*. **261** 221 (1996)
61. Kikuchi K et al. *J. Am. Chem. Soc*. **116** 9775 (1994)
62. Sueki K et al. *Chem. Phys. Lett*. **291** 37 (1998)
63. Sato W et al. *Phys. Rev. Lett*. **80** 133 (1998)
64. Haufler R E et al. *J. Phys. Chem*. **94** 8634 (1990)
65. Diederich F et al. *Science* **252** 548 (1991)
66. Michel R H et al., in *Physics and Chemistry of Fullerenes and Derivatives* (Eds H Kuzmany et al.) (Singapore: World Scientific, 1995) p. 89
67. Shinohara H et al. *J. Phys. Chem*. **97** 4259 (1993)
68. Shinohara H et al. *J. Phys. Chem*. **98** 2008 (1994)
69. Kikuchi K et al. *Chem. Phys. Lett*. **216** 67 (1993)
70. Stevenson S et al. *Anal. Chem*. **66** 2675; 2680 (1994)
71. Shinohara H et al., in *Recent Advances in the Chemistry and Physics of Fullerenes and Related Materials* (Proc. Electrochemical Society, Vol. 94-24, Eds K M Kadish, R S Ruoff) (Pennington, N.J.: Electrochemical Soc., 1994) p. 1361
72. Capp C et al. *J. Am. Chem. Soc*. **116** 4987 (1994)
73. Xiao J et al. *J. Am. Chem. Soc*. **116** 9341 (1994)
74. Savina M et al., in *Recent Advances in the Chemistry and Physics of Fullerenes and Related Materials* (Proc. Electrochemical Society, Vol. 94-24, Eds K M Kadish, R S Ruoff) (Pennington, N.J.: Electrochemical Soc., 1994) p. 1309
75. Kubozono Y et al. *Chem. Lett*. 457 (1995); 453 (1996); 1061 (1996)
76. Kubozono Y et al. *J. Am. Chem. Soc*. **118** 6998 (1996)
77. Yamamoto K et al. *J. Phys. Chem*. **98** 12831 (1994)
78. Fowler P W, Manolopoulos D E *An Atlas of Fullerenes* (Oxford: Clarendon Press, 1995)
79. Yamamoto E et al. *J. Am. Chem. Soc*. **118** 2293 (1996)
80. Nakane T et al., in *Molecular Nanostructures* (Eds H Kuzmany et al.) (Singapore: World Scientific, 1998) p. 193
81. Xu Z et al. *J. Am. Chem. Soc*. **118** 11309 (1996)
82. John T, Dennis S, Shinohara H *Appl. Phys. A* **66** 243 (1998)
83. Hennrich F H et al. *Angew. Chem. Int. Ed. Engl*. **35** 1732 (1996)
84. Dennis S, Shinohara H *Chem. Commun*. (1998)
85. Kirbach U, Dunsch L *Angew. Chem. Int. Ed. Engl*. **35** 2380 (1996); *Angew. Chem*. **108** 2518 (1996)
86. Shinohara H et al. *Mater. Sci. Forum*. **232** 207 (1966)
87. Nagase S, Kobayashi K, Akasaka T, in *Fullerenes and Fullerene Nanostructures* (Eds H Kuzmany et al.) (Singapore: World Scientific, 1996) p. 161
88. Weaver J H et al. *Chem. Phys. Lett*. **190** 460 (1992)
89. Poirier D M et al. *Phys. Rev. B* **49** 17403 (1994)
90. Kessler B et al. *Phys. Rev. Lett*. **79** 2289 (1997); in *Molecular Nanostructures* (Eds H Kuzmany et al.) (Singapore: World Scientific, 1998) p. 207
91. Pichler T et al., in *Molecular Nanostructures* (Eds H Kuzmany et al.) (Singapore: World Scientific, 1998) p. 211
92. Weidinger A et al., in *Electronic Properties of Novel Materials — Progress in Molecular Nanostructures* (AIP Conf. Proc., Vol. 442, Eds H Kuzmany et al.) (Woodbury, New York: AIP, 1998) p. 363
93. Mauser H, Clark T, Hirsch A, in *Electronic Properties of Novel Materials — Progress in Molecular Nanostructures* (AIP Conf. Proc., Vol. 442, Eds H Kuzmany et al.) (Woodbury, N.Y.: AIP, 1998) p. 392
94. Lu J, Zhang X, Zhao X *Chem. Phys. Lett*. **312** 85 (1999)
95. Kuran P et al. *Chem. Phys. Lett*. **292** 580 (1998)
96. Pichler T et al. *Appl. Phys. A* **66** 281 (1998)

97. Ding J, Yang S *J. Am. Chem. Soc.* **118** 11254 (1996)
98. Ding J et al. *Chem. Phys. Lett.* **261** 92 (1996)
99. Park C et al. *Chem. Phys. Lett.* **213** 196 (1993)
100. Rübsam M et al. *Chem. Phys. Lett.* **240** 615 (1995); in *Physics and Chemistry of Fullerenes and Derivatives* (Eds H Kuzmany et al.) (Singapore: World Scientific, 1995) p. 117
101. Shinohara H et al. *J. Phys. Chem.* **99** 13769 (1995)
102. Laasonen K, Andreoni W, Parrinello M *Science* **258** 1916 (1992)
103. Lin N et al. *J. Phys. Chem.* **102** 4411 (1998)
104. Hulman M et al., in *Electronic Properties of Novel Materials — Progress in Molecular Nanostructures* (AIP Conf. Proc., Vol. 442, Eds H Kuzmany et al.) (Woodbury, N.Y.: AIP, 1998) p. 378
105. Miyake Y *J. Phys. Chem.* **100** 9579 (1996)
106. Nagase S, Kobayashi K *J. Chem. Soc. Chem. Commun.* 1837 (1994)
107. Hummelen J C et al. *Science* **269** 1554 (1995)
108. Lamparts I et al. *Angew. Chem. Int. Ed. Engl.* **34** 2257 (1995)
109. Averdung J et al. *Tetrahedron* **51** 6977 (1995)
110. Akasaka T et al. *Chem. Lett.* 945 (1999)
111. Hummelen J S et al. *Science* **271** 1554 (1995)
112. Nuber B, Hirsch A *J. Chem. Soc., Chem. Commun.* 1421 (1996)
113. Bellavia-Lund C et al. *J. Am. Chem. Soc.* **119** 8101 (1997)
114. Gruss A et al. *J. Am. Chem. Soc.* **119** 8728 (1997)
115. Van Loosdrecht P et al. *Phys. Rev. Lett.* **73** 3415 (1994)
116. Kato T et al. *J. Phys. Chem.* **51** 13425 (1993)
117. Sato W et al. *Phys. Rev. B* **58** 10850 (1998)
118. Hasegawa Y et al. *Phys. Rev. B* **56** 6470 (1997)
119. Vorobyev V S, Eletskii A V *Chem. Phys. Lett.* **254** 263 (1996)
120. Fuchs D, Rietschel H, in *Fullerenes and Fullerene Nanostructures* (Eds H Kuzmany et al.) (Singapore: World Scientific, 1996) p. 186
121. Knorr S et al. *Appl. Phys. A* **66** 257 (1998); in *Molecular Nanostructures* (Eds H Kuzmany et al.) (Singapore: World Scientific, 1998) p. 211
122. Allen K, Hellman F *J. Chem. Phys.* **111** 5291 (1999)
123. Bethune D S et al., in *Progress in Fullerene Research. Int. Winterschool on Electronic Properties of Novel Materials, Austria, 1994* (Eds H Kuzmany et al.) (Singapore: World Scientific, 1994) p. 102
124. Beyers R H M et al. *Nature* (London) **370** 196 (1994)
125. Saito Y et al. *Phys. Rev. B* **48** 9182 (1993)
126. Muto S et al. *Philos. Mag. B* **67** 443 (1993)
127. Lin N et al. *Phys. Rev.* **58** 2126 (1998)
128. Takata M et al., in *Fullerenes and Fullerene Nanostructures* (Eds H Kuzmany et al.) (Singapore: World Scientific, 1996) p. 155
129. Heiney P A et al. *Phys. Rev. Lett.* **66** 2911 (1991)
130. David W I F et al. *Europhys. Lett.* **18** 219 (1992)
131. Ishibashi M et al. *Jpn. J. Appl. Phys.* **33** L1265 (1994)
132. Waiblinger M et al., in *Electronic Properties of Novel Materials — Progress in Molecular Nanostructures* (AIP Conf. Proc., Vol. 442, Eds H Kuzmany et al.) (Woodbury, N.Y.: AIP, 1998) p. 388
133. Akasaka T, Nagase S, Kobayashi K, in *Fullerenes and Fullerene Nanostructures* (Eds H Kuzmany et al.) (Singapore: World Scientific, 1996) p. 200
134. Akasaka T et al. *J. Chem. Soc. Chem. Commun.* 1343 (1995)
135. Akasaka T et al. *Tetrahedron* **52** 5015 (1995)
136. Suzuki T et al. *J. Am. Chem. Soc.* **117** 9606 (1995)
137. Akasaka T et al. *Angew. Chem. Int. Ed. Engl.* **34** 2139 (1995)
138. Akasaka T et al. *Nature* (London) **374** 600 (1995)
139. Weidinger A et al. *Appl. Phys. A* **66** 287 (1998)
140. McElvany S W *J. Phys. Chem.* **96** 4935 (1992)
141. Iijima S *Nature* (London) **354** 56 (1991)
142. Pederson M R, Broughton J Q *Phys. Rev. Lett.* **69** 2689 (1992)
143. Ajayan P M, Iijima S *Nature* (London) **361** 333 (1993)
144. Ebbesen T W *Phys. Today* **49** (6) 26 (1996)
145. Ebbesen T W *Ann. Rev. Mater. Sci.* **24** 235 (1994)
146. Ebbesen T W *J. Phys. Chem. Solids* **57** 951 (1996)
147. Tsang S C et al. *Nature* (London) **372** 159 (1994)
148. Tsang S C et al. *J. Chem. Soc. Chem. Commun.* 1803 (1995)
149. Saito Y et al. *Chem. Phys. Lett.* **212** 379 (1993)
150. Yosida Y *Appl. Phys. Lett.* **64** 3048 (1994)
151. Zhang G L *J. Appl. Phys.* **80** 579 (1996)
152. Loiseau A *Fullerene Science and Technology* **4** 1263 (1996)
153. Guerret-Piecourt C et al. *Nature* (London) **372** 761 (1994)
154. Dillon A C et al. *Nature* (London) **386** 377 (1997)
155. Smith B W, Monthioux M, Luzzi D E *Nature* (London) **396** 323 (1998)
156. Berteaux B et al. *Chem. Phys. Lett.* **310** 21 (1999)